FAMILIES OF KNOT FLOER HOMOLOGY THEORIES AND DEEPLY SLICE KNOTS

By

Tristan Wells

A DISSERTATION

Submitted to
Michigan State University
in partial fulfillment of the requirements
for the degree of

Mathematics—Doctor of Philosophy

2024

ABSTRACT

In this dissertation, we present the culmination of two projects, after an overview of the primary tool involved in the research, Heegaard Floer theory. In this overview, we discuss the origins of Heegaard Floer homology, an invariant associated to a Spin^c 3-manifold, as well as its flavors. We then present multiple flavors of knot Floer homology, a refinement of that theory.

The first project is a structural theorem for a family of knot invariants due to Dowlin. L-space knots are knots which admit surgeries that have simple Heegaard Floer homology and thin knots are ones whose knot Floer homology is concentrated in a single δ-grading. Each class of knots has well known knot Floer complexes. As such, we show that for L-space knots and thin knots, the theories that Dowlin constructed are a change of coefficients from an older theory, the minus flavor of knot Floer homology. Many supporting examples are shown in its final section. The proof uses a popular cancellation lemma for chain complexes with the special shapes involved.

The second project is a collaboration with McConkey, St. Clair, and Zhang. In this dissertation, we show that the Whitehead double of the dual knot to $1/n$ surgery on the knot 6_1 in the 3-sphere is deeply slice in a contractible 4-manifold. That is, it bounds a smoothly embedded disc in the manifold, but not in a collar neighborhood of its boundary, the surgered manifold. This is partial progress in answering one of the Kirby questions regarding nullhomotopic deeply slice knots, as referenced in earlier work of Klug and Ruppik. To prove our theorem, we make use of the immersed curves perspective of bordered Floer homology and knot Floer homology, which we introduce in previous sections.

ACKNOWLEDGEMENTS

I always wonder how it is that the preface or acknowledgements section of a work I read comes to such great length. How can it be that there are that many on a writer's mind when assuming a reflective stance on a job "well-done"? Yet, as I ponder this myself, a slew of names clamber for attention in my thoughts.

First and foremost, I am deeply indebted to both my mother and my father for their unending emotional, mental, and financial support, deliberate or subconscious. I cannot imagine a life without such a formidable structure to lean on. The remainder of my family comes next to mind, where perhaps not a single mote of discouragement can be found. My nearby grandparents in Grand Rapids provided so much that I hesitate to move away.

Next are those that I became close to along the way. One of my closest friends, Dan, has been solidly supportive in every way, and it has been an immense pleasure to spend these six years together as friends, roommates, travel partners, confidants, colleagues, and almost brothers. Something similar goes for my other roommates over the years: Bridget, Brita, Sydney, David, Jacob, Joe, and Steven. Then there are so many affiliated with the them, the university, or otherwise that I shant attempt to recall them here, save for my academic brethren: Chen and Chris S., who have been particularly integrated into both my work and home lives. Other colleagues who struggled with me include Danika, Chris P., Dean, Ivan, Rithwik, and Rob.

Third is the entirety of the support from faculty and staff at Michigan State University, from the janitorial staff to the administrative staff, and from Andy and Tsveta for all things teaching to, of course, my advisory committee: Effie, Teena, Matt S., and my advisor Matt H. Without Matt H., to guide my mathematical upbringing and all of their support in navigating this strange sort of professional world, I would have been lost long ago.

Finally come my personal friends. As one who frequents the world of online gaming, I have established a network of lifelong friends from both before my time at MSU and onward. These are not limited to but must include: Ryan "Mirtsauce", Austin "Spandex", "Megavin",

Caleb "Inky", JP "Hobo", Nick "Bawitdaba", Mal, Irvine, Dallas, Taylor, Tobias, and my wonderful girlfriend, my dearest Marissa "PiercingPath", who checked in with me every step of the way.

It was my hope to incorporate my voice as much as possible in this dissertation, but technical writing asserts its writing patterns. With luck, these meager paragraphs will lend a hand to what I hope is a gentle introduction for any reader before the onslaught of mathematical rigor and depth obscures my voice entirely. For this opportunity to write my own thanks, I am very grateful. I guess it is not so surprising authors spend time on the acknowledgements.

TABLE OF CONTENTS

CHAPTER 1

INTRODUCTION

Beginning in as simple terms as possible, the content of this dissertation is *low dimensional topology*, which is the study of manifolds of dimension four or less. For the uninitiated, an *n-manifold* can be thought of simply as a space which appears like "ordinary" space nearby. The easiest example is the Earth; a human walking on the Earth appears to have two primary directions to move in: East/West or North/South, like the ant in Figure 1.1. Consequently, we say that the 2-dimensional sphere is a 2-manifold. One of the main goals of low dimensional topology is to classify manifolds as best we can. To do this, we construct *invariants*, which are labels that do not change when looking at an equivalent manifolds, much like labeling objects by color. The better the invariant, the finer the classification of the objects.

There is a similar process for other topological objects, like *knots*. Roughly speaking, a knot is a twisted up piece of string tied end to end. One can easily imagine a complicated such object, like the first knot with six crossings displayed in Figure 1.1. Since the 1920s, topologists have been interested in knots, whether it is to tabulate them or discover implications for other manifolds. A formal definition appears in Chapter 2. The purpose of this dissertation is to study a particular family of knot invariants in Chapter 3, and apply another kind of knot invariant in Chapter 4.

More formally, in 2001, Ozsváth and Szabó introduced topological invariants of a 3-manifold paired with extra data, a Spin^c structure. To a pair, $(Y, \mathfrak{s})$, they associate the Heegaard Floer homology groups $\widehat{HF}(Y, \mathfrak{s})$, $HF^-(Y, \mathfrak{s})$, $HF^+(Y, \mathfrak{s})$, and $HF^\infty(Y, \mathfrak{s})$ [OS04d]. Henceforth, $HF^\circ(Y, \mathfrak{s})$ will refer to the groups agnostic of flavor. In a follow-up publication, Ozsváth and Szabó explore further the properties of these invariants [OS04c]. The Heegaard Floer homology groups enjoy many properties. First, the construction of the chain groups is combinatorial, coming from a Riemannian surface together with a set of curves and marked points, called a *Heegaard diagram*. As a result, computing the groups is reasonable. Second,
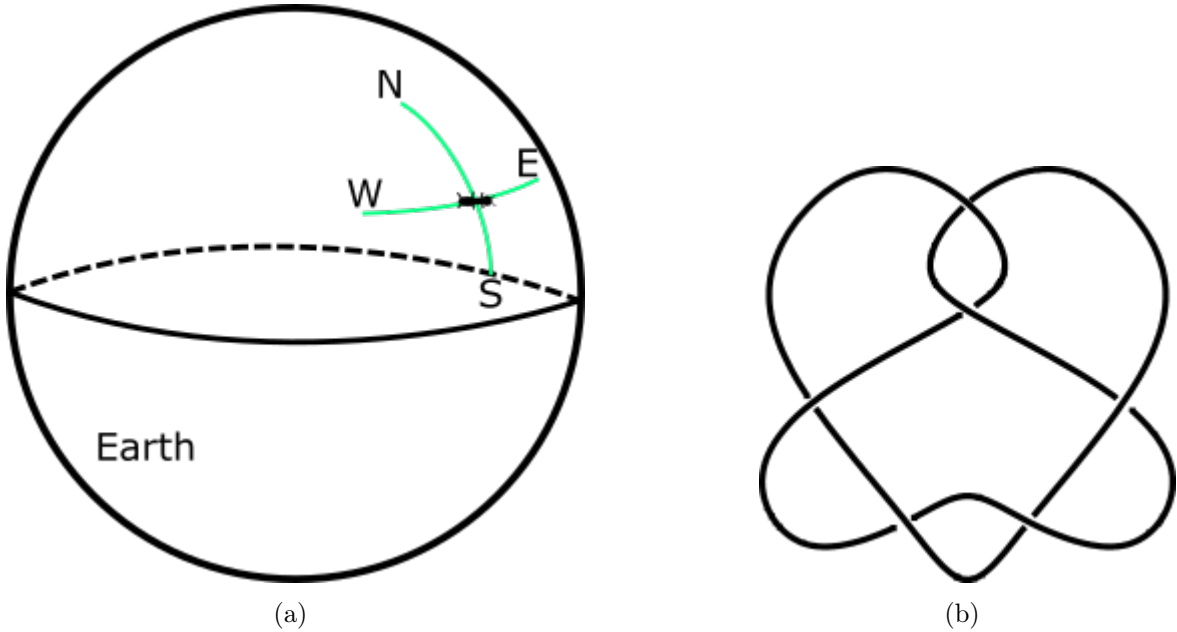
Figure 1.1 (a) A picture of the ant choosing between two directions on Earth's surface (a 2-sphere), and (b) a diagram depicting a possibly complicated twisted up piece of string, tied end to end, called a knot.

there are a number of exact triangles for the Heegaard Floer homology groups of 3-manifolds that differ by surgery on knots, yielding additional powerful computational tools [OS04c]. Finally, and most importantly for this dissertation, Ozsváth and Szabó in [OS04b], and independently Rasmussen in [Ras03], observed that a filtration of the chain complex for Heegaard Floer homology arising from the presence of a null-homologous knot in $(Y, \mathfrak{s})$ leads to a knot invariant called knot Floer homology.

At its core, knot Floer homology is the filtered chain homotopy type coming from a filtration associated to a null-homologous knot in Y. Roughly, the filtration comes from the Spin^c structures in the 3-manifold with boundary obtained by removing a neighborhood of the knot in Y. An extremely important property of knot Floer homology is that it *categorifies* a much older invariant, the Alexander polynomial. That is, the Alexander polynomial of a knot is the graded Euler characteristic of its knot Floer homology:

$$\Delta_K(t) = \sum_{\text{gr}_U, A} (-1)^{\text{gr}_U} t^A \text{rank} \widehat{HFK}_{\text{gr}_U}(K, A).$$

Since its advent, knot Floer homology has received extensive study, and is an essential com-

ponent to both projects presented here. Thus, the second chapter (Chapter 2) is dedicated to an overview of this theory.

Another knot invariant of active research is Khovanov homology, constructed by Khovanov in [Kho00]. Like knot Floer homology, the Khovanov homology groups can be computed combinatorially, although this time from a knot diagram. Also like knot Floer homology, Khovanov homology categorifies an older knot invariant, the Jones polynomial. That is, the Jones polynomial of a knot is the graded Euler characteristic of its Khovanov homology:

$$V_K(q) = \sum_{i,j}(-1)^i q^j \mathrm{rank} Kh_{i,j}(K).$$

Of particular interest are *spectral sequences* between invariants like Khovanov homology and Floer-theoretic invariants. In an effort to construct a spectral sequence between these two particular theories, Dowlin constructed a family of knot invariants which are obtained by taking quotients in the ground ring from the minus flavor of knot Floer homology, dubbed $HFK_n(K)$ [Dow18]. In Chapter 3, we prove a theorem regarding the structure of this family of invariants for two classes of knots:

Theorem 1.0.1. *If $K \subset S^3$ is an L-space knot or a thin knot, then*

$$HFK_n(K) \cong \left(HFK^-(K) \underset{\mathbb{Q}[U]}{\otimes} \frac{\mathbb{Q}[U]}{(U^n)}\right) \oplus \mathrm{Tor}_1^{\mathbb{Q}[U]}(HFK^-(K); \mathbb{Q}[U]).$$

To do this, we note that chain complexes arising from L-space knots and thin knots have special shapes [OS05a, Pet13]. *L-space* knots are ones which yield an L-space after *Dehn surgery* along the knot, a process discussed in Section 3.1.1. L-spaces are 3-manifolds whose Heegaard Floer homology is "simplest," i.e.

$$\mathrm{rank}\widehat{HF}(Y) = |H_1(Y; \mathbb{Z})|.$$

Thin knots are ones whose knot Floer homology is concentrated in a single δ-grading, where $\delta = \frac{1}{2}(\mathrm{gr}_U - \mathrm{gr}_V)$. Applications of a cancellation lemma on the level of chain complexes together with the universal coefficients theorem are the essential components of the proof.

Finally, Chapter 4 concerns a collaborative project with McConkey, St. Clair, and Zhang, where we outline a method of constructing *deeply slice* knots. These are knots in a 3-manifold Y which are smoothly slice in a 4-manifold with boundary Y, but not slice in a collar neighborhood of the boundary. That is, one can find a smoothly embedded disk in the 4-manifold that goes "deep" into the 4-manifold, but not otherwise. The main theorem in Chapter 4 is the following.

Theorem 1.0.2 (McConkey, St. Clair, W., Zhang). *For the first 6-crossing knot, $K = 6_1$, the Whitehead double of the dual knot to $1/n$ surgery along K, $D_+(\mu_{1/n}(K))$, is deeply slice in a contractible 4-manifold with boundary $S^3_{1/n}(K)$.*

The tools used in proving this theorem are extensive. We apply the results of Chen, Hanselman, Rasmussen, and Watson in various papers where they develop an immersed curves package for *bordered Heegaard Floer* homology [Che23, CH23, HRW23, HRW22]. Since background on this theory is involved, we present an overview in Section 4.2.

CHAPTER 2

HEEGAARD FLOER THEORY

The story underlying this dissertation began with the Heegaard Floer homology of closed Spin^c 3-manifolds, a theory which was refined in numerous ways for 3-manifolds with boundary. A capstone of these efforts, central to this dissertation, is the immersed curves perspective, which arose some two decades later.

2.1 Heegaard Floer Homology

The general machinery needed to construct the Heegaard Floer homology groups is rather extensive. For the purpose of self-containment, they are outlined here. However, proofs will be omitted and can be found in [OS04d] and [OS04a].

2.1.1 Heegaard Diagrams

The primary objects of study for Heegaard Floer homology are closed, oriented 3-manifolds. An essential object in Heegaard Floer theory is the idea of a *Heegaard diagram* representing a *Heegaard splitting*. A Heegaard splitting is a description of a closed 3-manifold as the union of two *genus g handlebodies* identified along their common boundary. It is well known that every closed 3-manifold admits a Heegaard splitting. A Heegaard diagram is a 2-dimensional way of encoding the information of a Heegaard splitting, which additionally gives a full handle decomposition of the 3-manifold.

Definition 2.1.1. A *genus g Heegaard diagram* for the 3-manifold $Y = H_\alpha \cup H_\beta$ is a closed, genus g surface F together with a set of g embedded simple closed curves $\boldsymbol{\alpha} = \{\alpha_1, ..., \alpha_g\}$, called the α-curves, which are linearly independent in $H_1(F; \mathbb{Z})$, and another set of g embedded simple closed curves $\boldsymbol{\beta} = \{\beta_1, ..., \beta_g\}$, called the β-curves, which are linearly independent in $H_1(F; \mathbb{Z})$ and intersect $\boldsymbol{\alpha}$ transversely.

To see the Heegaard splitting arising from the Heegaard diagram, thicken F to $F \times [0, 1]$ and attach a 3-dimensional 2-handle along each α-curve in $F \times \{0\}$. The result is a 3-manifold with two boundary components, one which is F and the other is a 2-sphere. Then there
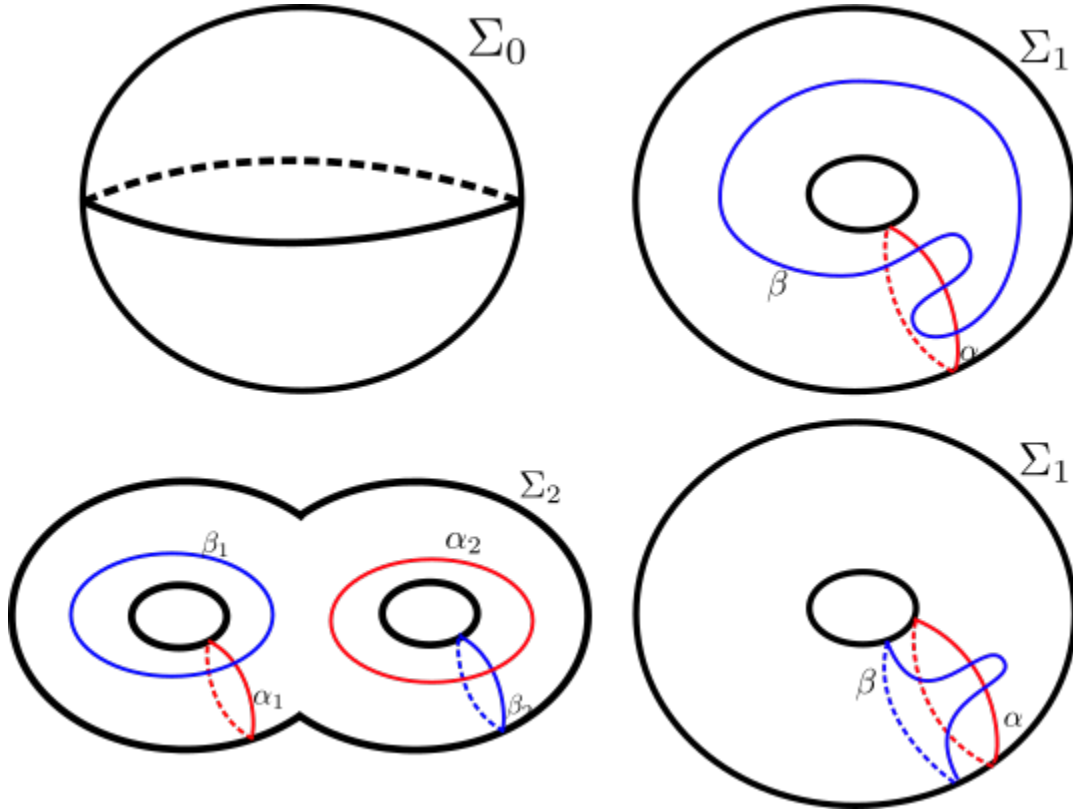
Figure 2.1 Top left: Genus 0 Heegaard diagram for S^3. Top right: Genus 1 Heegaard diagram for S^3 (stabilized from the left). Bottom left: Genus 2 Heegaard diagram for S^3. Bottom right: genus 1 Heegaard diagram for $S^1 \times S^2$.

is a unique way to attach a 3-ball to the 2-sphere boundary (up to orientation-preserving homeomorphism), yielding the handlebody H_α. Using the β-curves in $F \times \{1\}$ similarly yields the handlebody H_β. Regarding the α-curves as the belt circles of 3-dimensional 1-handles and the 3-ball as a 3-dimensional 0-handle yields a handle decomposition of Y. Some examples are shown in Figure 2.1.

Given a handle decomposition for Y, one can construct a *Morse function* $f : Y \to \mathbb{R}$ whose index i critical points (which are non-degenerate, isolated, and finite) correspond to attaching i-handles, and vise versa. The handlebodies in the Heegaard splitting of Y are $H_\alpha = f^{-1}\big([0, 3/2]\big)$ and $H_\beta = f^{-1}\big([3/2, 3]\big)$ and the Heegaard surface is $F = f^{-1}\big(\{3/2\}\big)$. More in depth descriptions of this process can be found in [GS99] and [Mil63], while a nice schematic is shown in Figure 2.2.
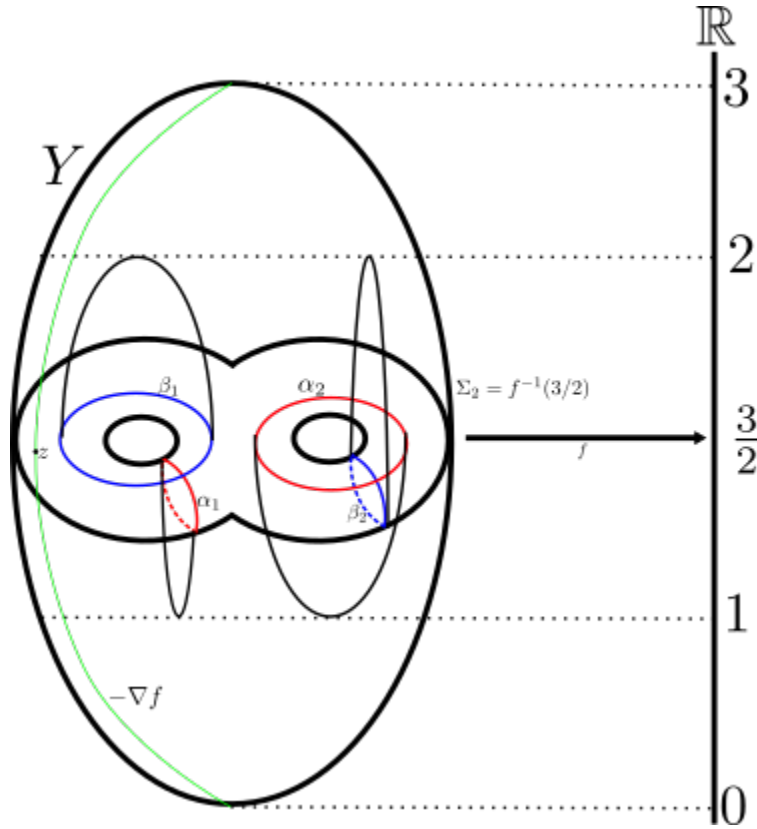
Figure 2.2 A schematic for the Morse function $f : S^3 \to \mathbb{R}$. The Heegaard surface, $\Sigma_g = f^{-1}(3/2)$, is shown in Figure 2.1. The attaching circles for H_α are in red, while the attaching circles for H_β are in blue. A gradient flow line (from top to bottom) is shown in green.

2.1.2   Heegaard Floer Chain Complex

Heegaard Floer homology can be interpreted as "infinite-dimensional Morse homology," which is nicely described in the lecture notes of Hutchings [Hut02]. Given a generic auxiliary metric on Y and a Morse function $f : Y \to \mathbb{R}$, consider the gradient flow lines of the gradient vector field $-\nabla f$ with respect to that metric. Then the Morse chain complex is roughly the graded $\mathbb{Z}$-module generated by critical points with the differential that counts the number of unparametrized flow lines between critical points that differ in index by one. Some flow lines are shown in Figure 2.2.

Recall that the Heegaard Floer groups are invariants of a 3-manifold Y together with a Spin^c structure, $\mathfrak{s}$. To account for $\mathfrak{s}$, a modification of the Heegaard diagram is in order.

7

Definition 2.1.2 (Heegaard Diagram). A *pointed genus g Heegaard diagram* for a closed, oriented 3-manifold Y is a tuple $(\Sigma_g, \boldsymbol{\alpha}, \boldsymbol{\beta}, w)$ where

- Σ_g is a closed, genus g surface,

- $\boldsymbol{\alpha}$ is a collection of g pairwise disjoint embedded simple closed curves on Σ_g which are linearly independent in $H_1(\Sigma_g; \mathbb{Z})$,

- $\boldsymbol{\beta}$ is a collection of g pairwise disjoint embedded simple closed curves on Σ_g which are linearly independent in $H_1(\Sigma_g; \mathbb{Z})$ and transverse to α,

- w is a basepoint in $\Sigma_g \setminus (\boldsymbol{\alpha} \cup \boldsymbol{\beta})$, and

- Y can be constructed as above from the data $(\Sigma_g, \boldsymbol{\alpha}, \boldsymbol{\beta})$ as in Definition 2.1.1.

Now we apply an analog of Morse homology, Lagrangian Floer homology, to the symmetric product of the Heegaard diagram. It is well known that $\mathrm{Sym}^g(\Sigma_g)$, the set of unordered g-tuples of points on Σ_g, is a $2g$-dimensional symplectic manifold which inherits a complex structure from a complex structure on Σ_g via the holomorphic quotient map $\Sigma_g^{\times g} \to \mathrm{Sym}^g(\Sigma_g)$. Then $\mathbb{T}_\alpha = \alpha_1 \times \alpha_2 \times \ldots \times \alpha_g$ and $\mathbb{T}_\beta = \beta_1 \times \beta_2 \times \ldots \times \beta_g$ are two Lagrangian submanifolds of $\mathrm{Sym}^g(\Sigma_g)$. Since $\boldsymbol{\alpha}$ and $\boldsymbol{\beta}$ intersect transversely, $\mathbb{T}_\alpha$ and $\mathbb{T}_\beta$ intersect transversely. In the Morse theoretic picture, the intersection points of the $\mathbb{T}_\alpha$ and $\mathbb{T}_\beta$ can be thought of as a g-tuple of gradient flow lines for f on Y, which pair up the index 2 and index 1 critical points.

Like the Morse chain complex, the Heegaard Floer chain complex is generated by these intersection points, and the differential counts "flow lines," in the form of pseudo-holomorphic discs between intersection points of index differing by 1. To see if there is such a disc between intersection point $\mathbf{x} \in \mathbb{T}_\alpha \cap \mathbb{T}_\beta$ and $\mathbf{y}$, one checks the homology class of the loop created by the gradient flow lines from $\mathbf{x}$ to $\mathbf{y}$ and back again. Through the equivalence

$$H_1(Y; \mathbb{Z}) \cong \frac{H_1(\Sigma_g; \mathbb{Z})}{\mathrm{span}\{[\boldsymbol{\alpha}], [\boldsymbol{\beta}]\}},$$
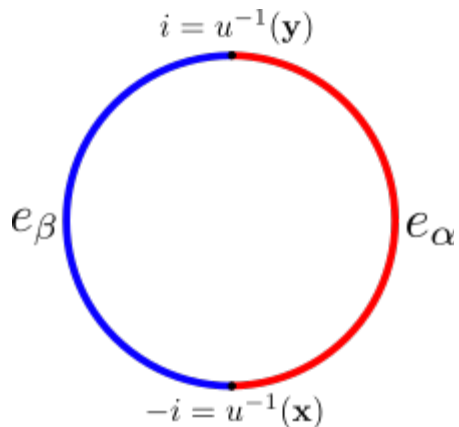
8

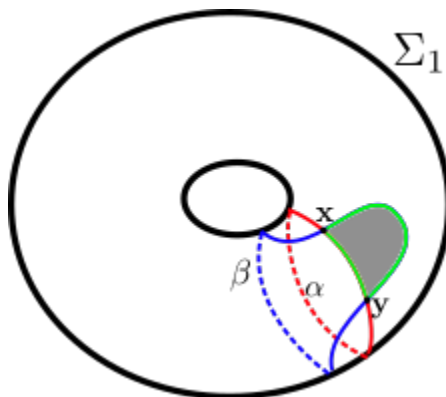Figure 2.3 A Whitney disc thought of as the unit disc in the complex plane.

Figure 2.4 A figure depicting a loop between x and y with $\epsilon(\mathbf{x}, \mathbf{y}) = 0$, in green.

the desired loop can be seen on Σ_g as a collection of arcs in $\boldsymbol{\alpha} \cup \boldsymbol{\beta}$ connecting the components of $\mathbf{x}$ and $\mathbf{y}$ in a particular way. For an example, see Figure 2.4. Given $\mathbf{x}$ and $\mathbf{y}$, let $\epsilon(\mathbf{x}, \mathbf{y})$ be the image of a loop connecting $\mathbf{x}$ and $\mathbf{y}$ in $H_1(Y; \mathbb{Z})$. We say $\mathbf{x} \sim \mathbf{y}$ if $\epsilon(\mathbf{x}, \mathbf{y}) = 0$. Thus, there is a (possibly empty) equivalence class of intersection points in $\mathbb{T}_\alpha \cap \mathbb{T}_\beta$ for each element of $H_1(Y, \mathbb{Z})$.

The group $H_1(Y, \mathbb{Z})$ is in one-to-one correspondence with the Spin^c structures on Y. Through Turaev's equivalence, on can regard the latter as homology classes of vector fields on Y outside a Euclidean ball [Tur97]. While many details of this equivalence are omitted, the choice of basepoint w distinguishes a flow line in Y of $-\nabla f$ from the index 3 critical point to the index 0 critical point, so that an intersection point $\mathbf{x} \in \mathbb{T}_\alpha \cap \mathbb{T}_\beta$ along with w fixes a Spin^c structure on Y. Thus, we have a map $\mathfrak{s}_w : \mathbb{T}_\alpha \cap \mathbb{T}_\beta \to \mathrm{Spin}^c(Y)$. There is a

Whitney disc between $\mathbf{x}$ and $\mathbf{y}$ when $\mathfrak{s}_w(\mathbf{x}) = \mathfrak{s}_w(\mathbf{y})$, or equivalently, when $\epsilon(\mathbf{x}, \mathbf{y}) = 0$.

Here, by a *Whitney disc* between $\mathbf{x}$ and $\mathbf{y}$, we mean a map from the unit disc in $\mathbb{C}$ to the symmetric product, $u : \mathbb{D} \to \mathrm{Sym}^g(\Sigma_g)$ such that $u(-i) = \mathbf{x}, u(i) = \mathbf{y}$, and the imaginary arc, e_α, of the boundary of the disc is mapped to an arc in $\mathbb{T}_\alpha$ and the real arc, e_β, is mapped to an arc in $\mathbb{T}_\beta$, as in Figure 2.3. Let $\pi_2(\mathbf{x}, \mathbf{y})$ be the set

$$\left[\left(\mathbb{D}, e_\alpha, e_\beta, -i, i \right), \left(\mathrm{Sym}^g(\Sigma_g), \mathbb{T}_\alpha, \mathbb{T}_\beta, \mathbf{x}, \mathbf{y} \right) \right].$$

This set $\pi_2(\mathbf{x}, \mathbf{y})$ is empty if $\epsilon(\mathbf{x}, \mathbf{y}) \neq 0$. Given $\phi \in \pi_2(\mathbf{x}, \mathbf{y})$, let $\mathcal{M}(\phi)$ be the moduli space of holomorphic representatives of ϕ. Let $\mu(\phi)$ be its expected dimension, called the *Maslov index* of ϕ. $\mathcal{M}(\phi)$ admits a natural $\mathbb{R}$ action by translation by looking at a Whitney disc as a vertical strip. $\widehat{\mathcal{M}}(\phi) = \mathcal{M}(\phi)/\mathbb{R}$ is a compact manifold of dimension 0 when $\mu(\phi) = 1$. Let $n_w(\phi)$ denote the algebraic intersection between ϕ and the subvariety $\{w\} \times \mathrm{Sym}^{g-1}(\Sigma_g)$.

We now have everything in place to define the Heegaard Floer complex:

Definition 2.1.3. Given a closed, smooth 3-manifold Y together with a Spin^c structure $\mathfrak{s}$ and a Heegaard diagram $(\Sigma_g, \boldsymbol{\alpha}, \boldsymbol{\beta}, w)$ for Y, the *Heegaard Floer chain complex* of $(Y, \mathfrak{s})$ is freely generated over $\mathbb{F}[U, U^{-1}]$ by all intersection points $\mathbf{x} \in \mathbb{T}_\alpha \cap \mathbb{T}_\beta$ such that $\mathfrak{s}_w(\mathbf{x}) = \mathfrak{s}$, denoted

$$CF^\infty(Y, \mathfrak{s}; \mathbb{F}[U, U^{-1}]) := \bigoplus_{\substack{\mathbf{x} \in \mathbb{T}_\alpha \cap \mathbb{T}_\beta \\ \mathfrak{s}_w(\mathbf{x}) = \mathfrak{s}}} \mathbb{F}[U, U^{-1}],$$

with boundary map defined on generators by

$$\partial^\infty(\mathbf{x}) := \sum_{y \in \mathbb{T}_\alpha \cap \mathbb{T}_\beta} \sum_{\substack{\phi \in \pi_2(x, y) \\ \mu(\phi) = 1}} \#\widehat{\mathcal{M}}(\phi) U^{n_w(\phi)} \mathbf{y}.$$

Theorem 2.1.4. *[OS04d]* $CF^\infty(Y, \mathfrak{s}; \mathbb{F}[U, U^{-1}])$ *is a chain complex, i.e.* $(\partial^\infty)^2 = 0$.

Since we will see that the homology of this complex is an invariant later, we ignore the dependence of the above definition on the Heegaard diagram (a slight abuse of notation). Notice that when $\mathbb{F} = \mathbb{Z}/2\mathbb{Z}$, $\widehat{\mathcal{M}}(\phi)$ is either 0 or 1. Henceforth, $\mathbb{F}$ will be taken to be

the field of two elements to avoid discussion of signs. The *Heegaard Floer groups* of $(Y, \mathfrak{s})$ are the homology groups of various subcomplexes of $CF^\infty(Y, \mathfrak{s})$. After a discussion about gradings, we present the theorems (without proof) necessary to establish the homology of $CF^\infty(Y, \mathfrak{s}, \mathbb{F}[U, U^{-1}])$ as a 3-manifold invariant.

2.1.3 Gradings and Flavors

The complex in Definition 2.1.3 comes equipped with a relative integral grading, called the *Maslov grading*, defined on generators with $\pi_2(\mathbf{x}, \mathbf{y}) \neq 0$ by:

$$\mathrm{gr}(\mathbf{x}) - \mathrm{gr}(\mathbf{y}) = \mu(\phi) - 2n_w(\phi).$$

For an arbitrary choice of grading 0, we can now define the subcomplex $CF^-(Y, \mathfrak{s}) \subset CF^\infty(Y, \mathfrak{s})$ generated by all $\mathbf{x}$ with negative Maslov grading, and its quotient complex $CF^+(Y, \mathfrak{s})$.

As $\mathbb{F}[U]$-modules, they each admit an action via multiplication by U which lowers the Maslov grading by 2. The kernel of this action yields another subcomplex, $\widehat{CF}(Y, \mathfrak{s})$, which can be thought of as the subquotient where the differential only counts discs which have no algebraic intersection with the subvariety $\{w\} \times \mathrm{Sym}^{g-1}(\Sigma_g)$, i.e. $n_w(\phi) = 0$. Each variant, dubbed $CF^\circ(Y, \mathfrak{s})$ when not specifying the flavor, has an induced differential, and their associated homology groups $HF^\circ(Y, \mathfrak{s})$ are the homology groups of the corresponding chain complex. The following essential theorem holds:

Theorem 2.1.5 ([OS04d]). *The invariants $HF^\circ(Y, \mathfrak{s})$ thought of as modules over $\mathbb{F}[U]$, are topological invariants of Y and $\mathfrak{s}$ in that they are independent of choice of Heegaard diagram and choice of path of almost complex structures $\mathrm{Sym}^g(\Sigma_g)$.*

The preceding theorem is proven by showing invariance under pointed *Heegaard moves* consisting of isotopies of curves (maintaining some kind of admissibility conditions), handle slides, and (de)stabilizations, all of which occur in the compliment of the basepoint w.

2.1.4 Examples

It is illuminating to consider a common example computation of Heegaard Floer homology for S^3, omitting only the most technical details. Using the genus 1 diagram in Figure 2.1 will allow us to look for discs in the 1-fold symmetric product of the torus, which is still just the torus. In general, counting discs using the data of the Heegaard diagram is quite difficult. Other tools have been developed to make computations easier and more combinatorial, such as the methods in [SW10], [MOT09], and [LOT14], the latter of which is closely related to methods in Section 4.2.

Let us look more closely at a genus 1 Heegaard diagram for S^3 in Figure 2.5. Since Σ_g is just the torus ($g = 1$), $\mathbb{T}_\alpha$ and $\mathbb{T}_\beta$ are simply the curves α and β respectively. The Heegaard Floer chain complex $\widehat{CF}(S^3)$ is generated by the intersection points a, b, and c of α and β. We can see immediately from considering the loops on Σ_g that $\epsilon(a,c) = \epsilon(b,c) = \epsilon(b,c) = 0$, which aligns with the fact that S^3 admits only a single Spin^c structure, corresponding to 0 in its first homology. Although discussion on how to determine the Maslov index of a disc has been omitted, it is the case that any disc from a to c does not have Maslov index 1. However, the discs labeled ϕ_1 and ϕ_2 have $\mu(\phi_1) = \mu(\phi_2) = 1$, and will be counted in differentials. Following the formulae in Definition 2.1.3, the differentials are

$$\widehat{\partial}(a) = 0 \qquad\qquad \partial^-(a) = 0$$

$$\widehat{\partial}(b) = c \qquad\qquad \partial^-(b) = Ua + c$$

$$\widehat{\partial}(c) = 0 \qquad\qquad \partial^-(c) = 0.$$

Taking homology for the hat flavor, we see that the generators b and c have an arrow canceling them, so $\widehat{HF}(S^3) \cong \mathbb{Z}/2\mathbb{Z} = \mathbb{F}_2$, generated by a. For the minus flavor, we again see that b cancels with the linear combination $Ua + c$, leaving a as the sole generator of $HF^-(S^3) \cong \mathbb{F}_2[U]$.
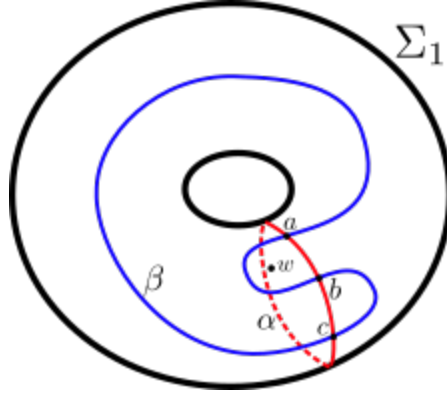
Figure 2.5 A "standaard" genus 1 pointed Heegaard diagram for S^3, where the beta (blue) curve β is perturbed to give more intersection points.

2.2 Knot Floer Homology

Having introduced the machinery of Heegaard Floer homology, most of the tools needed to construct a Heegaard Floer-theoretic invariant for knots in S^3 are in place. First, let us establish some preliminaries. A null-homologous *knot* in a 3-manifold Y is an isotopy class of embeddings $K : S^1 \hookrightarrow Y$ such that $[K] = 0 \in H_1(Y; \mathbb{Z})$. The manifold of primary concern in this paper is S^3, in which all circle embeddings are null-homologous, henceforth, "knot" will mean an isotopy class of embeddings of S^1 in S^3, and will be denoted simply by K. Often, a knot is depicted by projecting it to the 2-sphere and recording crossing information at the double points (for a generic projection). This is called a *knot diagram*, and a few examples of knot diagrams are shown in Figure 2.6. One important knot is the so-called unknot, $\mathcal{U}$, which is the only knot which has a knot diagram with no crossings and is isotopic to the unit circle in the equator S^2 of S^3. A long-standing goal of low-dimensional topologists and knot theorists is to tabulate and classify all the knots in S^3, among discerning their other properties. One such tool, which also yields interesting results in 3- and 4-manifold topology is knot Floer homology, a refinement of Heegaard Floer homology to an invariant pairs (S^3, K). As in Section 2.1, many proofs and details may be omitted, but found in [OS04b] or [Ras03].

Figure 2.6 Left: A knot diagram of the unknot. Middle: Another knot diagram of the unknot. Right: A knot diagram of the trefoil.

2.2.1 Doubly-pointed Heegaard Diagrams

To refine the Heegaard Floer homology groups to invariants of the pair (S^3, K), we need to add extra data to Heegaard diagrams for S^3. In particular, we define the following:

Definition 2.2.1 (Doubly-pointed Heegaard diagram)**.** A *doubly-pointed Heegaard diagram* for S^3 compatible with a knot $K \hookrightarrow S^3$ is a tuple $(\Sigma_g, \boldsymbol{\alpha}, \boldsymbol{\beta}, w, z)$ where

- $(\Sigma_g, \boldsymbol{\alpha}, \boldsymbol{\beta}, w)$ is a Heegaard diagram for S^3 as in Definition 2.1.2, and

- z is another basepoint in $\Sigma_g \setminus (\boldsymbol{\alpha} \cup \boldsymbol{\beta})$ such that K can be recovered from w and z.

The recovery of the knot is as follows: Using the Heegaard splitting of S^3 into H_α and H_β as in Section 2.1.1, connect w to z by a curve on $\Sigma_g \setminus \boldsymbol{\alpha}$ and push the curve into H_α. Similarly, connect z to w by a curve on $\Sigma_g \setminus \boldsymbol{\beta}$ and push it into H_β. The result is an embedding of K into the described 3-manifold, in this case, S^3. From a Morse theoretic perspective, the knot K can be thought of as a union of two gradient flow lines of $-\nabla f$ from the index 3 critical point to the index 0 critical point, specified by the z and w basepoints, where $f : S^3 \to \mathbb{R}$ is the Morse function giving rise to the Heegaard diagram $(\Sigma_g, \boldsymbol{\alpha}, \boldsymbol{\beta}, w, z)$. It is well known that any knot in S^3 (or any 3-manifold) admits a compatible doubly-pointed Heegaard diagram. Figure 2.7 depicts a common Heegaard diagram for the trefoil.

2.2.2 Knot Floer Complexes

The additional basepoint not only records the isotopy type of the knot, but also induces a filtration on the complex $CF^\infty(S^3)$, called the *Alexander filtration*: Given generators $\mathbf{x}$ and $\mathbf{y}$
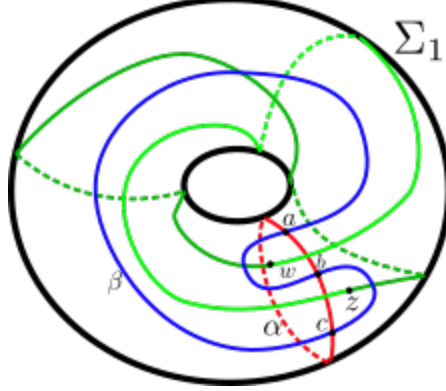
Figure 2.7 A doubly-pointed Heegaard diagram compatible with the trefoil in S^3. The green arcs make up the knot.

for $CF^\infty(S^3)$ and a disc $\phi \in \pi_2(\mathbf{x}, \mathbf{y})$, their Alexander filtration level differs by $n_z(\phi) - n_w(\phi)$.

Definition 2.2.2. Given a knot K in S^3 and a doubly-pointed Heegaard diagram $\mathcal{H} = (\Sigma_g, \boldsymbol{\alpha}, \boldsymbol{\beta}, w, z)$ compatible with K, the *full knot Floer complex* of the pair (S^3, K) is freely generated over $\mathbb{F}[U, V]$ by all intersection points $\mathbf{x} \in \mathbb{T}_\alpha \cap \mathbb{T}_\beta$, denoted

$$CFK_{U,V}(K) := \bigoplus_{\mathbf{x} \in \mathbb{T}_\alpha \cap \mathbb{T}_\beta} \mathbb{F}[U, V],$$

with boundary map defined on generators by

$$\partial^{U,V}(\mathbf{x}) := \sum_{y \in \mathbb{T}_\alpha \cap \mathbb{T}_\beta} \sum_{\substack{\phi \in \pi_2(x,y) \\ \mu(\phi)=1}} \#\widehat{\mathcal{M}}(\phi) U^{n_w(\phi)} V^{n_z(\phi)} \mathbf{y}.$$

As before, we will see that the invariants derived from this complex do not depend on the Heegaard diagram, so we often (slightly abusively) write $CFK_{U,V}(K)$ in place of $CFK_{U,V}(\mathcal{H})$. In fact,

Theorem 2.2.3 ([OS04b])**.** *The chain homotopy type of $CFK_{U,V}(K)$ is a topological invariant of (S^3, K) in that it is independent of choice of Heegaard diagram.*

As before, the proof checks invariance under Heegaard moves. Also like before, the modules carry grading information. The obvious first choice is to allow the naive bi-grading by U and V on the ring $\mathbb{F}[U, V]$ to descend to a relative grading on the full knot Floer

complex. The bi-grading $\mathrm{gr} = (\mathrm{gr}_U, \mathrm{gr}_V)$ is such that $\mathrm{gr}(U) = (-2, 0)$ and $\mathrm{gr}(V) = (0, -2)$. Then the Alexander grading is defined to be $A = \frac{1}{2}(\mathrm{gr}_U - \mathrm{gr}_V)$. The inherited relative gradings on $CFK_{U,V}(K)$ for $\phi \in \pi_2(\mathbf{x}, \mathbf{y})$ mimic the relative grading on $CF^\infty(S^3)$:

$$\mathrm{gr}_U(\mathbf{x}) - \mathrm{gr}_U(\mathbf{y}) = \mu(\phi) - 2n_w(\phi)$$

$$\mathrm{gr}_V(\mathbf{x}) - \mathrm{gr}_V(\mathbf{y}) = \mu(\phi) - 2n_z(\phi).$$

Setting $V = 1$ and remembering only gr_U recovers the definition of $CF^-(S^3)$ as in Section 2.1.4. Choosing the grading of 1 in $HF^-(S^3) \cong \mathbb{F}[U]$ to be 0 establishes an absolute U grading on $CFK_{U,V}(K)$. This process is simply forgetting the new basepoint, z. Forgetting w instead has a symmetrical effect, and establishes the absolute V grading on $CFK_{U,V}(K)$. This symmetry will be an essential computational tool much later, in Chapter 4.

2.2.3 Flavors

As is the case in Heegaard Floer homology, the filtered complexes also enjoy many variations. Since the chain homotopy type of $CFK_{U,V}(K)$ is invariant, all of the following restrictions are as well. First, setting $U = V = 0$ gives a chain complex over $\mathbb{F}$ with the restriction in the differential that one only counts discs which do not intersect either basepoint. We denote this complex, the *knot Floer homology*, by $\widehat{CFK}(K) = \bigoplus_{\mathbf{x} \in \mathbb{T}_\alpha \cap \mathbb{T}_\beta} \mathbb{F}\langle \mathbf{x} \rangle$ with the induced differential

$$\widehat{\partial}(\mathbf{x}) := \sum_{y \in \mathbb{T}_\alpha \cap \mathbb{T}_\beta} \sum_{\substack{\phi \in \pi_2(x,y) \\ \mu(\phi)=1 \\ n_w(\phi)=n_z(\phi)=0}} \#\widehat{\mathcal{M}}(\phi)\mathbf{y}.$$

Another choice is to only set $V = 0$, yielding a chain complex over $\mathbb{F}[U]$ with the restriction in the differential being that one only counts discs which do not intersect the z basepoint, but can intersect the w basepoint. We denote this complex, the *minus flavor* of knot Floer homology, by $CFK^-(K) = \bigoplus_{\mathbf{x} \in \mathbb{T}_\alpha \cap \mathbb{T}_\beta} \mathbb{F}[U]$ with the induced differential

$$\partial^-(\mathbf{x}) = \sum_{y \in \mathbb{T}_\alpha \cap \mathbb{T}_\beta} \sum_{\substack{\phi \in \pi_2(x,y) \\ \mu(\phi)=1 \\ n_z(\phi)=0}} \#\widehat{\mathcal{M}}(\phi)U^{n_w(\phi)}\mathbf{y}.$$

16

In both cases, it is more common to prescribe the bi-grading on the modules with gr_U and A, which sacrifices no information since any two gradings among gr_U, gr_V, and A determine the third. These complexes are $\mathbb{Z} \oplus \mathbb{Z}$-filtered complexes by powers of U and V, and it is most convenient to present a filtered complex information in the integral lattice with the Alexander filtration on the vertical axis and the algebraic filtration coming from the U action on the horizontal axis, as in Figure 2.8.

2.2.4 Examples

We will now flesh out an example using the Heegaard diagram for S^3 in Figure 2.5. First, we refine the Heegaard diagram with the extra data coming from the trefoil knot in S^3, which we denote $T_{2,3}$ since it's the $p = 2, q = 3$ torus knot. The resulting diagram and knot are shown in Figure 2.7. Using this, we can compute the modules and differentials for various flavors of knot Floer homology. Let us consider $CFK^-(T_{2,3})$ and $\widehat{CFK}(T_{2,3})$. Each are modules over their respective rings with three generators, a, b, and c. The differentials, following the definitions above are

$$\partial^{U,V}(a) = 0 \qquad\qquad \widehat{\partial}(a) = 0 \qquad\qquad \partial^-(a) = 0$$

$$\partial^{U,V}(b) = Ua + Vc \qquad\qquad \widehat{\partial}(b) = 0 \qquad\qquad \partial^-(b) = Ua$$

$$\partial^{U,V}(c) = 0 \qquad\qquad \widehat{\partial}(c) = 0 \qquad\qquad \partial^-(c) = 0.$$
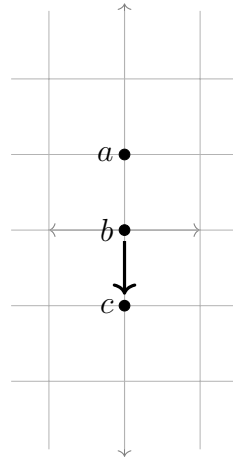
It is convenient to look at these complexes in the plane in order to take homology and keep track of gradings, using Figure 2.8. Now it is plain to see that $\widehat{HFK}(T_{2,3}) \cong \mathbb{F}_{(0,1)} \oplus \mathbb{F}_{(-1,0)} \oplus \mathbb{F}_{(-2,-1)}$, where $\widehat{\mathrm{gr}} = (\mathrm{gr}_U, A)$. Similarly, $HFK^-(T_{2,3}) \cong \mathbb{F}_{(0,1)} \oplus \mathbb{F}[U]_{(-2,-1)}$, where the $\mathbb{F}$ summand is generated by a and the $\mathbb{F}[U]$ summand is generated by c and powers of U times c.
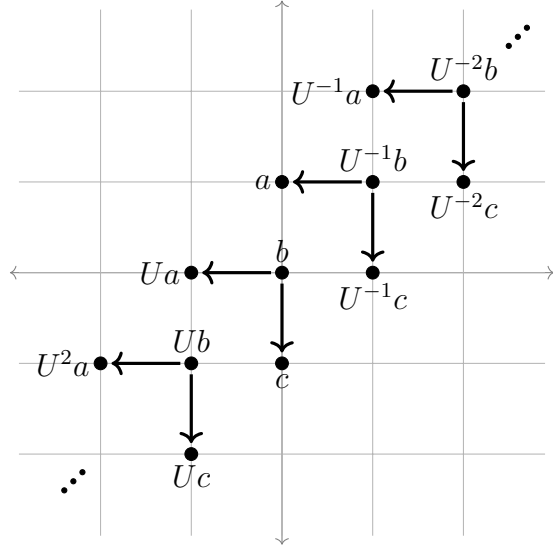
(a) $CFK^\infty(T_{2,3})$
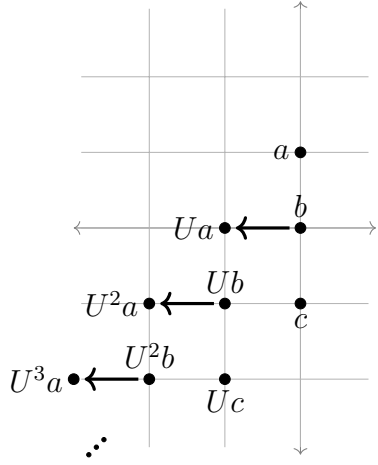
(b) $gCFK^-(T_{2,3})$

(c) $\widehat{CFK}(T_{2,3})$

Figure 2.8 A bunch of versions of the knot Floer complex for the trefoil.

CHAPTER 3

A STRUCTURE THEOREM FOR A FAMILY OF KNOT FLOER HOMOLOGY THEORIES

The relationship between the Floer-theoretic knot invariants introduced by Ozsváth and Szabó [OS04b] and Rasmussen [Ras03] and the quantum knot invariants of Khovanov [Kho00] and Khovanov and Rozansky [ML04, KR08] has been an active topic in topology for the past twenty years. These invariants categorify many knot invariants, like the Jones polynomial and the Alexander polynomial. That is, the graded Euler characteristic of these theories returns the respective polynomials. The first such relationship came from a spectral sequence from the Khovanov homology of a link to the Heegaard Floer homology of its double branched cover, constructed by Ozsváth and Szabó in [OS05b]. Since then, a slew of spectral sequences of that form have been discovered, yielding a variety of rank inequalities between the associated homologies as well as indicating the possibility of more interesting relationships.

The following was a long-standing conjecture of Rasmussen from [Ras05]:

Theorem 3.0.1 (Rasmussen's Conjecture, [Dow24]). *For a knot $K \subset S^3$, $rk(Kh(K)) \geq rk(\widehat{HFK}(K))$.*

In [Ras05], Rasmussen suggests that constructing a spectral sequence is a promising way to address this conjecture, a strategy successfully employed by Dowlin in [Dow18, Dow24]. It is natural to want to complete the diagram in Figure 3.1 with spectral sequences from the Khovanov-Rozansky homologies, $KR_n(K)$, to a proposed Floer-theoretic analog. In [Dow18], Dowlin defines a candidate family of knot invariants, called $HFK_n(K)$, and presents the generalized conjecture.

Conjecture 3.0.2. [Dow18] For a knot $K \subset S^3$, there are spectral sequences $KR_n(K) \rightrightarrows HFK_n(K)$ and $\overline{KR_n}(K) \rightrightarrows \widehat{HFK_n}(K)$.

Motivated by Conjecture 3.0.2, we study $HFK_n(K)$, and make the following conjecture.
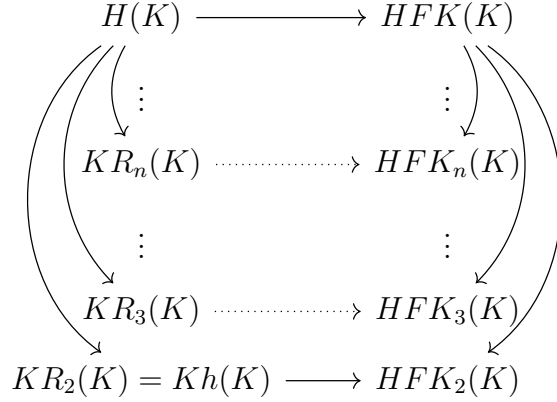
$$H(K) \longrightarrow HFK(K)$$

$$\vdots \qquad\qquad \vdots$$

$$KR_n(K) \dashrightarrow HFK_n(K)$$

$$\vdots \qquad\qquad \vdots$$

$$KR_3(K) \dashrightarrow HFK_3(K)$$

$$KR_2(K) = Kh(K) \longrightarrow HFK_2(K)$$

Figure 3.1 Dotted arrows are conjectured, while solid arrows have been proven in suitable versions.

Conjecture 3.0.3. For any knot K (or more generally, link) in S^3, $HFK_n(K)$ can be obtained by a change of coefficients from $HFK^-(K)$.

Although further investigation is required to prove Conjecture 3.0.3, much can be said about two wide classes of knots for which the knot Floer homology (among other invariants) is already well understood and computable. In particular, we focus our attention on *L-space knots* and *Floer homologically thin knots*.

3.1 Surgery and L-Space Knots

3.1.1 Dehn Surgery

One ubiquitous way to describe a 3-manifold is via *Dehn surgery* on a knot or link in S^3. Since knots are smooth embeddings, any $K \subset S^3$ has a *tubular neighborhood*, $\nu(K)$, which, after cutting S^3 open by removing $\nu(K)$, can be identified with the solid torus, a genus 1 handlebody whose boundary is the "standard" torus, denoted T^2. This can be seen in Figure 3.2. We then have two 3-manifolds with boundary: $\nu(K)$ and the *knot exterior*, $S^3 \setminus \mathring{\nu}(K)$, sometimes denoted X_K. Their boundaries are $\partial(S^3 \setminus \nu(K)) = \partial\nu(K) = T^2$. For further details, see [Sav11].

Now that there has been some cutting, it is only natural to do some gluing. It is immediately clear that identifying the common boundary of $S^3 \setminus \nu(K)$ and $\nu(K)$ will return S^3, but other gluings via homeomorphisms of T^2 are also possible. We say Y is obtained
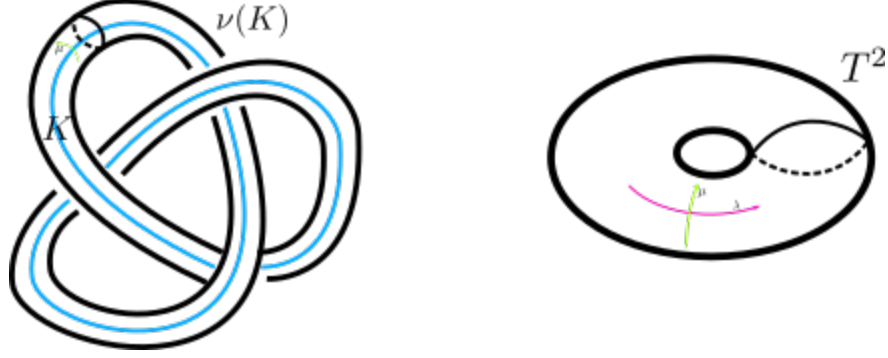
Figure 3.2 Left: A knot in S^3 with a regular tubular neighborhood. Right: the standard solid torus, with preferred basis for $H_1(\partial(\nu(K)) = T^2$ labeled as λ and μ.

from *surgery along* K in S^3 if it was obtained by removing a neighborhood of K and gluing the boundaries of $S^3 \setminus K$ and $\nu(K)$ via a homeomorphism of T^2, $h : T^2 \to T^2$. That is, $Y = S^3 \setminus K \cup_h \nu(K)$. This idea can be extended to links by doing knot surgery on each component consecutively.

The resulting manifold depends entirely on h. Even further, one only needs to keep track of the image of the *meridian* of K, called μ, thought of as $\{point\} \times \partial \mathbb{D} \in T^2$. Up to isotopy, any simple closed curve on T^2 can be given by a pair of coprime integers (p, q), keeping track of its homology class in $H_1(T^2; \mathbb{Z})$ in the basis given by a certain *longitude* of K in $S^3 \setminus \nu(K)$ and the meridian of K. This longitude, called the *Seifert longitude*, λ, is the curve on $\partial(S^3 \setminus \nu(K))$ which is homologically trivial in $S^3 \setminus \nu(K)$. Then Y depends only on $\left[h(\{point\} \times \partial \mathbb{D}) \right] = p\mu + q\lambda \in H_1(\partial S^3 \setminus \nu(K))$, where either p or q could be 0. It is well known that any closed orientable 3-manifold can be obtained by surgery on some link in S^3, and we often write $Y = S^3_{p/q}(K)$ for the reduced fraction $p/q \in \mathbb{Q} \cup \{\infty\}$ to indicate the surgery.

3.1.2 L-Space Complexes

The Heegaard Floer homology of L-spaces are particularly well understood. A rational homology 3-sphere Y is an *L-space* if $\mathrm{rk}\widehat{HF}(Y) = |H_1(Y)|$. A knot is a positive (or negative) *L-space knot* if it admits a positive (or negative, respectively) surgery ($p/q > 0$) yielding an L-space. We think of L-spaces as having the "simplest" Heegaard Floer homology possible.
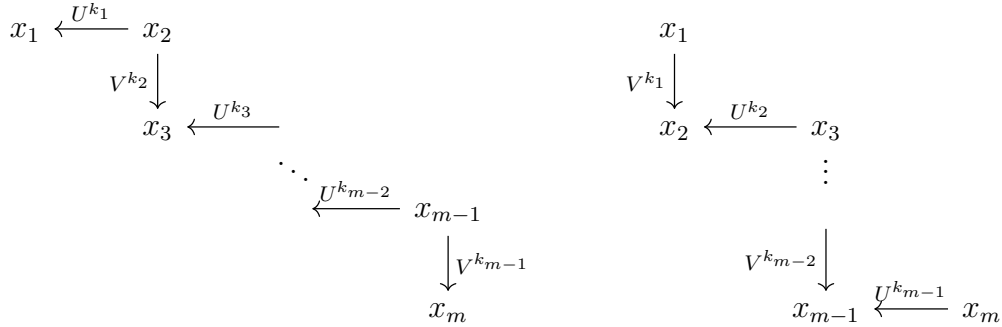
Figure 3.3 Plotted roughly in the integral lattice given by gr_U and gr_V, the left shows a positive staircase complex, while the right shows a negative staircase complex.

A summand frequently appearing in the full knot Floer complex of highly studied knots is the so-called staircase complex:

Definition 3.1.1 (Staircase)**.** A chain complex $C = \bigoplus_{i=1}^{m} \mathbb{F}[U, V]$ freely generated by $\{x_i\}_{i=1}^{m}$ is a *staircase complex* if it is in one of the forms in Figure 3.3 for some positive integers k_i and odd integer $m \geq 3$, where each x_i is the generator of $\mathbb{F}[U, V]$ corresponding to the i-th summand of C.

With the following theorem, we see that staircase complexes completely characterize L-space knot Floer homology:

Theorem 3.1.2 ([OS05a])**.** *If a knot K is a positive (or negative) L-space knot, then $CFK^-(K)$ is chain homotopy equivalent to a positive (or negative, respectively) staircase complex.*

The full knot Floer complex for the trefoil, $CFK_{U,V}(T_{2,3})$ as in an example in Section 2.2.4, is a staircase complex.

3.2 Thin Knots and the δ-Grading

Recall from Section 2.2.2 that full knot Floer complexes are birgraded modules by (gr_U, A). There is a combination of these gradings, called the *δ-grading*, given by

$$\delta = A - \mathrm{gr}_U.$$

This can be thought of as a relative δ-grading on $CFK_{U,V}(K)$ in the following way. Given a doubly-pointed Heegaard diagram for $K \subset S^3$ and $\phi \in \pi_2(\mathbf{x}, \mathbf{y})$, the relative δ-grading is

$$\delta(\mathbf{x}) - \delta(\mathbf{y}) = n_z(\phi) + n_w(\phi) - \mu(\phi).$$

A knot K is *Floer homologically thin*, or just *thin*, if its knot Floer homology is supported in a single δ-grading. For example, we know from the trefoil example in Section 2.2.4 that

$$\widehat{HFK}(T_{2,3}) \cong \mathbb{F}_{(0,-1)} \oplus \mathbb{F}_{(1,0)} \oplus \mathbb{F}_{(2,1)}.$$

The δ-gradings of $1 \in \mathbb{F}$ in each summand are all -1, so the knot Floer homology of the right-handed trefoil is thin.

Like L-space knots, thin knot Floer complexes have a nice form. There is another model summand to include:

Definition 3.2.1 (Box). A chain complex $C = \bigoplus_{i=1}^{4} \mathbb{F}[U, V]$ freely generated by $\{x_i\}_{i=1}^{4}$ is a *box complex* if it is in the form

$$
\begin{array}{ccc}
x_2 & \xleftarrow{\ U^k\ } & x_1 \\
{\scriptstyle V^l}\big\downarrow & & \big\downarrow{\scriptstyle -V^l} \\
x_4 & \xleftarrow{\ U^k\ } & x_3
\end{array}
$$

for some positive integers k and l, where each x_i is the generator of $\mathbb{Q}[U, V]$ corresponding to the i-th summand of C.

Theorem 3.2.2 ([Pet13]). *If a knot K is Floer homologically thin, then $CFK^-(K)$ is a direct sum of box and staircases complexes each of which consist only of arrows with all U and V powers equal to 1.*

3.3 The Family $HFK_n(K)$

In an effort to fill in the right side of Figure 3.1, Dowlin defined a family of Floer-theoretic knot invariants meant to enjoy similar properties to the Khovanov-Rozansky homology theories. Indeed, the forthcoming invariants, $HFK_n(K)$, have many properties beyond invariance. For a detailed description, see [Dow18], as many proofs will be omitted here. For

completeness, the original definition for these invariants for links in an arbitrary 3-manifold is presented. A *link* in a 3-manifold Y is simply a knot of multiple components, i.e. an isotopy class of embeddings $L : \sqcup S^1 \hookrightarrow Y$. The discussion will begin with links in mind, but quickly be constrained to the case when the link has only one component, i.e. a knot.

3.3.1 Heegaard Diagrams

Once again, a modification of the Heegaard diagram Definition 2.2.1 is needed to include the link information:

Definition 3.3.1. A (multi-pointed) *Heegaard diagram* $\mathcal{H}$ for a link L in a closed, oriented 3-manifold Y is the data $(\Sigma_g, \boldsymbol{\alpha}, \boldsymbol{\beta}, \mathbf{w}, \mathbf{z})$ where

- Σ_g is a closed, oriented, genus g surface, called the Heegaard surface.

- $\boldsymbol{\alpha}$ (respectively, $\boldsymbol{\beta}$) is a set of $g + k - 1$ disjoint embedded circles $\{\alpha_1, ..., \alpha_{g+k-1}\}$ (resp. $\{\beta_1, ..., \beta_{g+k-1}\}$) in Σ such that the alpha curves intersect the beta curves transversely.

- $\boldsymbol{\alpha}$ and $\boldsymbol{\beta}$ each span a g-dimensional subspace of $H_1(\Sigma_g; \mathbb{Z})$, and

- $\mathbf{w}$ and $\mathbf{z}$ are each sets of k basepoints $\{w_1, ...w_k\}$ and $\{z_1, ..., z_k\}$ such that each component of $\Sigma_g \setminus \boldsymbol{\alpha}$ and each component of $\Sigma_g \setminus \boldsymbol{\beta}$ contains a $\mathbf{w}$ basepoint and a $\mathbf{z}$ basepoint.

As before, the manifold Y is constructed from this data by thickening Σ_g to $\Sigma_g \times [0, 1]$ and attaching thickened discs along the alpha curves at $\Sigma_g \times \{0\}$ and along the beta curves at $\Sigma_g \times \{1\}$ and then filling in the resulting 2-sphere boundaries (now multiple) with 3-balls. The link L in Y can be seen as follows. When thickening Σ_g, also thicken the $\mathbf{w}$ and $\mathbf{z}$ basepoints to get arcs $\mathbf{w} \sqcup \mathbf{z} \times [0, 1] \subset \Sigma_g \times [0, 1]$. Since each component of $\Sigma_g \setminus \boldsymbol{\alpha}$ has a $\mathbf{w}$ and $\mathbf{z}$ basepoint, we connect those arcs in $\mathbf{w} \sqcup \mathbf{z} \times [0, 1]$ with an arc in the 3-ball attached to that component's S^2 boundary. We do this similarly for the $\Sigma \times \{1\}$ boundaries.

Dowlin extended this notion to a *punctured Heegaard diagram* which adds to $\mathcal{H}$ the following data:

- a basepoint p, called the *puncture*, and

- curves α_{g+k} and β_{g+k} which bound discs, and which separate p from the **w** and **z** basepoints, such that $\boldsymbol{\alpha}$ and $\boldsymbol{\beta}$ still intersect transversely and span a g-dimensional subspace of $H_1(\Sigma_g; \mathbb{Z})$.

Puncturing the Heegaard diagram is like considering $L \sqcup \mathcal{U}$ (where $\mathcal{U}$ is the unknot) where the unlinked unknot has only a single basepoint p. This is just a $(0,3)$-stabilization in the sense of [OS04b].

3.3.2 Complexes

The first construction needed is, in some sense, the widest one can think of to extrapolate the full knot Floer complex in Section 2.2.2. In fact, the following is not even a chain complex in general, without identifications in the ground ring or restrictions on the link. In addition, we make all definitions henceforth in this chapter with the ground field the rationals, $\mathbb{Q}$, since Dowlin's work requires it.

Definition 3.3.2. Given a multi-pointed Heegaard diagram $\mathcal{H} = (\Sigma_g, \boldsymbol{\alpha}, \boldsymbol{\beta}, \mathbf{w}, \mathbf{z})$ compatible with L, the *master knot Floer complex* of the pair (Y, L) is

- the $\mathbb{Q}[U, V]$-module freely generated by all intersection points $\mathbf{x} \in \mathbb{T}_\alpha \cap \mathbb{T}_\beta$, denoted

$$CFK_{U,V}(\mathcal{H}) := \bigoplus_{\mathbf{x} \in \mathbb{T}_\alpha \cap \mathbb{T}_\beta} \mathbb{Q}[U, V],$$

- and the boundary map given by counting the Maslov index 1 pseudo-holomorphic discs from one intersection point to the others, denoted (using subscripts to distinguish it from Definition 2.2.2)

$$\partial_{U,V}(\mathbf{x}) = \sum_{\mathbf{y} \in \mathbb{T}_\alpha \cap \mathbb{T}_\beta} \sum_{\substack{\phi \in \pi_2(\mathbf{x}, \mathbf{y}) \\ \mu(\phi)=1}} \#\widehat{\mathcal{M}}(\phi) U_1^{n_{w_1}(\phi)} ... U_k^{n_{w_k}(\phi)} V_1^{n_{z_1}(\phi)} ... V_k^{n_{z_k}(\phi)} \mathbf{y}.$$

In general, $CFK_{U,V}(\mathcal{H})$ is not a true chain complex, as mentioned, but a curved one. Let $w_{a(i)}$ be the **w** basepoint connected to z_i via an arc in H_α, and $w_{b(i)}$ be the arc connected to z_i via an arc in H_β. Then the curved complex has potential

$$\partial_{U,V}^2 = \sum_{i=1}^{k} (U_{a(i)} - U_{b(i)}) V_i.$$

When each component of L has exactly one $\mathbf{w}$ and $\mathbf{z}$ basepoint, $CFK_{U,V}(\mathcal{H})$ is a true complex, since $a(i) = b(i)$ for the singular value of i.

As with other algebraic variations on complexes involving two formal variables, Dowlin makes a particular one to define a family of complexes:

Definition 3.3.3 ([Dow18]). Given a multi-pointed Heegaard diagram $\mathcal{H}$ for a link L in a 3-manifold Y, define the chain complexes $CFK_n(\mathcal{H})$ to be the quotient

$$CFK_n(\mathcal{H}) = CFK_{U,V}(\mathcal{H}) \Big/ \left(V_i - \frac{U_{a(i)}^n - U_{b(i)}^n}{U_{a(i)} - U_{b(i)}} \right),$$

and the differential ∂_n is the induced differential from $\partial_{U,V}$. If there is only one basepoint w and one basepoint z, define

$$CFK_n(\mathcal{H}) = CFK_{U,V}(\mathcal{H}) \Big/ \left(V - nU^{n-1} \right).$$

Together with the following theorems, $HFK_n(L) = H_*(CFK_n(\mathcal{H}))$ where $\mathcal{H}$ is any punctured Heegaard diagram for L, are invariants of the pair (Y, L).

Theorem 3.3.4 ([Dow18]). *The map $\partial_n : CFK_n(\mathcal{H}) \to CFK_n(\mathcal{H})$ satisfies $\partial_n^2 = 0$.*

Theorem 3.3.5 ([Dow18]). *If $\mathcal{H}_1$ and $\mathcal{H}_2$ are two punctured Heegaard diagrams with k curves for a null-homologous link L, then $CFK_n(\mathcal{H}_1)$ and $CFK_n(\mathcal{H}_2)$ are chain homotopy equivalent as $\mathbb{Q}[U_1, ..., U_k]$-modules.*

We perform some computations in Section 3.5. These examples illustrate that, for knots, one has a simpler equivalent definition of $HFK_n(K)$. In fact, in the case where $L = K$ is a knot, $HFK_n(K)$ can be computed from $CFK_{U,V}(K)$ without a punctured Heegaard diagram. Dowlin presents an alternate definition, which he proves is equivalent in the following theorem.

Theorem 3.3.6 ([Dow18]). *If $\mathcal{H}$ is an unpunctured diagram for a knot K in S^3 with a single pair of basepoints w and z, then*

$$HFK_n(K) = H_*\left(\frac{CFK_{U,V}(\mathcal{H})}{(UV, V - nU^{n-1})}\right).$$

3.4 Structure Theorem

Since $\mathbb{Q}[U]$ is a principal ideal domain,

$$H_*\left(CFK^-(K) \underset{\mathbb{Q}[U]}{\otimes} \frac{\mathbb{Q}[U]}{(U^n)}\right) \cong \left[H_*\left(CFK^-(K); \mathbb{Q}[U]\right) \underset{\mathbb{Q}[U]}{\otimes} \frac{\mathbb{Q}[U]}{(U^n)}\right] \oplus \operatorname{Tor}_1^{\mathbb{Q}[U]}(HFK^-(K); \mathbb{Q}[U]).$$

This fact motivates Conjecture 3.0.3 as well as the idea for the following algebraic machinery.

Recall that Dowlin's definition of the complex $CFK_n(K)$ for knots in Theorem 3.3.6 is the quasi-isomorphism

$$CFK_n(K) \cong \frac{CFK_{U,V}(K)}{(UV, V - nU^{n-1})}.$$

In the examples later in Section 3.5, this complex turns out to be isomorphic to

$$\widetilde{CFK}_n(K) := CFK^-(K) \underset{\mathbb{Q}[U]}{\otimes} \frac{\mathbb{Q}[U]}{(U^n)}$$

which we can compute using the universal coefficient theorem. This leads to another definition:

Definition 3.4.1. Given a chain complex of free $\mathbb{Q}[U,V]$-modules $C = \bigoplus \mathbb{Q}[U,V]$, define the $\mathbb{Q}[U]$-modules

$$C_n := \frac{C}{(UV, V - nU^{n-1})}$$
$$\widetilde{C}_n := \frac{C}{(V, U^n)}.$$

Notice that

$$\frac{C}{(UV, V - nU^{n-1})} \cong C \underset{\mathbb{Q}[U,V]}{\otimes} \frac{\mathbb{Q}[U,V]}{(UV, V - nU^{n-1})},$$

$$
\begin{array}{ccc}
x_1 & x_2 & x_3 \\
Ux_1 & Ux_2 & Ux_3 \\
U^2x_1 & U^2x_2 & U^2x_3 \\
\vdots & \vdots & \vdots \\
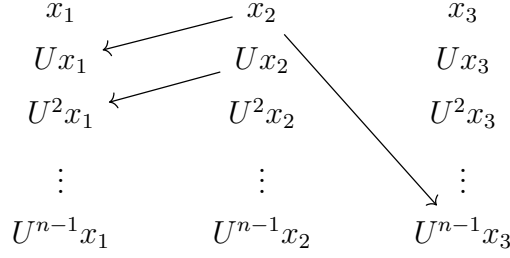U^{n-1}x_1 & U^{n-1}x_2 & U^{n-1}x_3
\end{array}
$$

Figure 3.4 The tower (vector space) structure of the complex $CFK_n(T_{2,3})$ (the complex shown in Figure 3.7).For example, $\partial_n(x_2) = Ux_1 + nU^{n-1}x_3$ and $\partial_n(Ux_2) = U^2x_1$.

and similarly that

$$
\frac{C}{(V, U^n)} \cong C \underset{\mathbb{Q}[U,V]}{\otimes} \frac{\mathbb{Q}[U,V]}{(V, U^n)} \cong \frac{C}{(V)} \underset{\mathbb{Q}[U]}{\otimes} \frac{\mathbb{Q}[U]}{(U^n)},
$$

so $CFK_n(K)$ and $\widetilde{CFK}_n(K)$ are as in Definition 3.4.1.

Given a chain complex C over $\mathbb{Q}[U, V]$, we often have Figure 3.4 in mind for the complexes C_n and $\widetilde{C}_n$. Each generator corresponding to a summand has a tower of chains, and the differential is marked by arrows between them. Figure 3.4 shows $CFK_n(T_{2,3})$. This structure also clearly shows C as a $\mathbb{Q}$-vector space.

In general, C_n and $\widetilde{C}_n$ are not isomorphic as $\mathbb{Q}[U, V]$-modules or quasi-isomorphic, while they are isomorphic as $\mathbb{Q}[U]$-modules. In fact, we have the following counterexample:

Lemma 3.4.2. C_n and $\widetilde{C}_n$ do not always have the same homology.

Proof. Consider the complex C given by

$$
\mathbb{Q}[U, V] \xrightarrow{V} \mathbb{Q}[U, V].
$$

Then C_n is

$$
\frac{\mathbb{Q}[U]}{(U^n)} \xrightarrow{nU^{n-1}} \frac{\mathbb{Q}[U]}{(U^n)}
$$

and $\widetilde{C}_n$ is

$$
\frac{\mathbb{Q}[U]}{(U^n)} \xrightarrow{0} \frac{\mathbb{Q}[U]}{(U^n)}.
$$

On the level of homology,

$$
H_*(C_n) \cong \frac{\mathbb{Q}[U]}{(U^{n-1})} \oplus \frac{\mathbb{Q}[U]}{(U^{n-1})}
$$

$$
H_*(\widetilde{C}_n) \cong \frac{\mathbb{Q}[U]}{(U^n)} \oplus \frac{\mathbb{Q}[U]}{(U^n)}.
$$

$$x_2 \xleftarrow{\;U^k\;} x_1$$

$$\left\downarrow{nU^{n-1}}\right. \qquad \left\downarrow{-nU^{n-1}}\right.$$

$$x_4 \xleftarrow{\;U^k\;} x_3$$

$$x_2 \xleftarrow{\;U^k\;} x_1$$

$$\left\downarrow{0}\right. \qquad \left\downarrow{0}\right.$$

$$x_4 \xleftarrow{\;U^k\;} x_3$$

Figure 3.5 On the left: C_n for $l = 1$. On the right: $\widetilde{C}_n$ for $l = 1$.

$\square$

To prove the main theorem of this chapter, we employ the following algebraic lemmata.

Lemma 3.4.3 (Cancellation lemma, [HN13]). *Let (C, ∂) be a chain complex of $\mathcal{R}$-modules, freely generated by chains $\{x_i\}$, and suppose that $d(x_k, x_l)$ is a unit in $\mathcal{R}$, where*

$$\partial(x_k) = \sum_{m \neq l} a_m x_m + d(x_k, x_l)x_l.$$

Then we can define a complex (C', ∂'), freely generated by $\{x_i | i \neq k, i \neq l\}$, which is chain homotopy equivalent to (C, ∂).

Lemma 3.4.4. *For any box complex C, $H_*(C_n) \cong H_*(\widetilde{C}_n)$ is an isomorphism of $\mathbb{Q}[U]$-modules.*

Proof. Any box complex can be pictorially represented as in Definition 3.2.1. Note that after the identifications $V = nU^{n-1}$ and $UV = 0$ in the ground ring, if $l > 1$,

$$V^l = V \cdot V^{l-1}$$

$$= nU^{n-1}V^{l-1}$$

$$= UV \cdot nU^{n-2}V^{l-2}$$

$$= 0.$$

So we see that if $l > 1$, the vertical arrows become zero in both C_n and $\widetilde{C}_n$, and $C_n = \widetilde{C}_n$. Thus, we restrict our attention to when $l = 1$. In this case, C_n and $\widetilde{C}_n$ are as in Figure 3.5. By direct computation using a similar diagram to Figure 3.4,

$$H_*(C_n) \cong \left(\frac{\mathbb{Q}[U]}{(U^k)}\right)^4 \cong H_*(\widetilde{C}_n).$$

$\square$

29

Lemma 3.4.5. *For any staircase complex C, $H_*(C_n) \cong H_*(\widetilde{C}_n)$ is an isomorphism of $\mathbb{Q}[U]$-modules.*

Proof. Any staircase complex can be pictorially represented as in Definition 3.1.1. We break the proof into a case for each type of staircase.

Case 1: The staircase is like the left in Figure 3.3. Using a similar argument as in the proof of Lemma 3.4.4, we can restrict our attention to the even i for which $k_i = 1$, which are the only places C_n and $\widetilde{C}_n$ differ. Regarding C_n and $\widetilde{C}_n$ as $\mathbb{Q}$-vector spaces (and, as such, $\mathbb{Q}$-modules), we have that $\partial_n x_i = U^{k_{i-1}} x_{i-1} + n U^{n-1} x_{i+1}$. Since $d(x_i, U^{k_{i-1}} x_{i-1}) = 1$, finite applications of Lemma 3.4.3 yield a chain homotopy equivalent complex of $\mathbb{Q}$-modules, $\overline{C}_n$, where the generators $U^{k_{i-1}} x_{i-1}$ and x_i are removed. A visual representation of the cancellations are as in Figure 3.6. After cancelling the same arrows in $\widetilde{C}_n$, the resulting chain complex is equal to $\overline{C}_n$ as in Figure 3.6. We can readily compute $H_*(C_n)$ and $H_*(\widetilde{C}_n)$ by computing $H_*(\overline{C}_n)$. The complex $\overline{C}_n$ is simply $\frac{m-1}{2}$ towers coming in pairs of the form in Figure 3.6, with arrows given by multiplication by $U^{k_{i-1}}$ for even i, and one single tower with no arrows for $i = m$. Thus,

$$H_*(\overline{C}_n) = \bigoplus_{s=1}^{\frac{m-1}{2}} \left(\frac{\mathbb{Q}[U]}{(U^{k_{2s-1}})} < x_{2s-1} > \oplus \frac{\mathbb{Q}[U]}{(U^{k_{2s-1}})} < U^{n-k_{2s-1}} x_{2s} > \right) \oplus \frac{\mathbb{Q}[U]}{(U^n)} < x_m > .$$

Case 2: The staircase is like the right in Figure 3.3. The argument is exactly the same as in case 1, except we now restrict our attention to the odd i for which $K_i = 1$, and we apply Lemma 3.4.3 on the generator pairs $(U^{n-1} x_{i+1}, U^{n-k_{i+1}-1} x_{i+2})$ for such i. The new complex $\overline{C}_n$ is still $\frac{m-1}{2}$ towers coming in pairs of the form in Figure 3.6, but now with arrows given by multiplication by $U^{k_{i-1}}$ for *odd* i, and the singular tower with no arrows is at $i = 1$.

In both cases, to see the isomorphism of $\mathbb{Q}[U]$-modules, we check how U acts on homology. Indeed, the distinction in module structures arose from the V-action on C, but the U-action remains unchanged throughout. □

The main theorem of this chapter is the following structural theorem for the shape of $HFK_n(K)$:
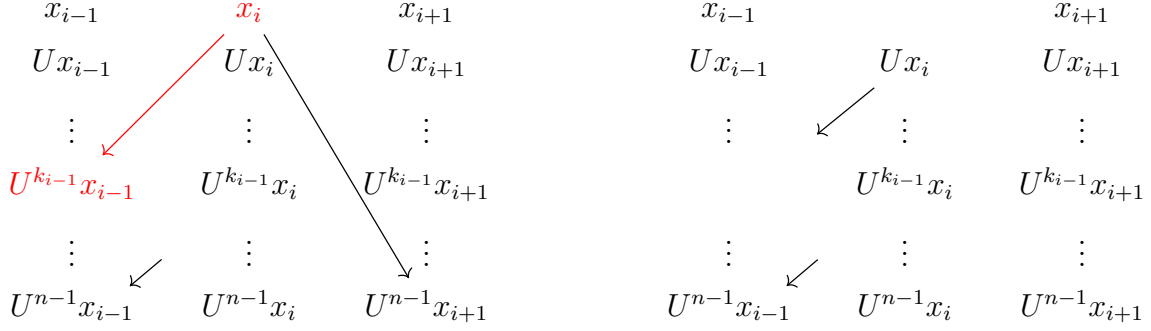
Figure 3.6 A local picture of a cancellation for some even i where $k_i = 1$. On the left: the cancelled arrow appears in red in the complex C_n. On the right: the new complex, $\overline{C_n}$, which is chain homotopy equivalent to C_n.

Theorem 3.4.6. *If $K \subset S^3$ is an L-space knot or a thin knot, then*

$$HFK_n(K) \cong \left(HFK^-(K) \underset{\mathbb{Q}[U]}{\otimes} \frac{\mathbb{Q}[U]}{(U^n)}\right) \oplus \mathrm{Tor}_1^{\mathbb{Q}[U]}(HFK^-(K); \mathbb{Q}[U]).$$

Proof. The argument is a chain of isomorphisms given by Lemmata 3.4.5, 3.4.4, and the universal coefficient theorem. The universal coefficient theorem says

$$H_*\!\left(CFK^-(K) \underset{\mathbb{Q}[U]}{\otimes} \frac{\mathbb{Q}[U]}{(U^n)}\right) \cong \left[H_*\!\left(CFK^-(K); \mathbb{Q}[U]\right) \underset{\mathbb{Q}[U]}{\otimes} \frac{\mathbb{Q}[U]}{(U^n)}\right] \oplus \mathrm{Tor}_1^{\mathbb{Q}[U]}(HFK^-(K); \mathbb{Q}[U]).$$

But

$$HFK^-(K) = H_*(CFK^-(K))$$

and Lemmata 3.4.5 and 3.4.4 yield

$$HFK_n(K) \cong H_*\!\left(CFK^-(K) \underset{\mathbb{Q}[U]}{\otimes} \frac{\mathbb{Q}[U]}{(U^n)}\right).$$

Piecing it all together gives the result. $\qquad\qquad\square$

3.5 Examples

3.5.1 Trefoil

As mentioned above, $CFK_{U,V}(T_{p,q})$ can be read off from its Alexander polynomial. For the trefoil, it is well-known that $\Delta(T_{2,3}) = t^{-1} - 1 + t$. Since the spacing between the powers of t are only one each, we have only a single power of U and V as the maps on the complex,

$$\mathbb{Q}[U] \xleftarrow{\;U\;} \mathbb{Q}[U] \qquad\qquad \frac{\mathbb{Q}[U]}{(U^n)} \xleftarrow{\;U\;} \frac{\mathbb{Q}[U]}{(U^n)}$$

$$\downarrow 0 \qquad\qquad\qquad\qquad\qquad \downarrow nU^{n-1}$$

$$\mathbb{Q}[U] \qquad\qquad\qquad\qquad \frac{\mathbb{Q}[U]}{(U^n)}$$

Figure 3.7 On the left: the complex $CFK^-(T_{2,3})$. On the right: the complex $CFK_n(T_{2,3})$.

yielding the usual staircase picture:

$$\mathbb{Q}[U,V] \xleftarrow{\;U\;} \mathbb{Q}[U,V]$$

$$\downarrow V$$

$$\mathbb{Q}[U,V]$$

The complex $CFK_n(T_{2,3})$ looks the same with the appropriate quotients. Both $CFK^-(K)$ and $CFK_n(K)$ are pictured in Figure 3.7. On the level of homology, we see the following:

$$HFK_n(T_{2,3}) \cong \frac{\mathbb{Q}[U]}{(U^n)} \oplus \mathbb{Q} \oplus \mathbb{Q}$$

$$HFK^-(T_{2,3}) \cong \mathbb{Q}[U] \oplus \mathbb{Q}.$$

Notice that since $\mathrm{Tor}_1^{\mathbb{Q}[U]}(\mathbb{Q} \oplus \mathbb{Q}[U], \frac{\mathbb{Q}[U]}{(U^n)}) \cong \mathbb{Q}$, by the universal coefficient theorem,

$$HFK_n(T_{2,3}) \cong HFK^-(T_{2,3}) \underset{\mathbb{Q}[U]}{\otimes} \frac{\mathbb{Q}[U]}{(U^n)} \bigoplus \mathrm{Tor}_1^{\mathbb{Q}[U]}(HFK^-(T_{2,3}); \mathbb{Q}[U])$$

$$\cong (\mathbb{Q}[U] \oplus \mathbb{Q}) \underset{\mathbb{Q}[U]}{\otimes} \frac{\mathbb{Q}[U]}{(U^n)} \bigoplus \mathbb{Q}$$

$$\cong \frac{\mathbb{Q}[U]}{(U^n)} \oplus \mathbb{Q} \oplus \mathbb{Q}.$$

We see similar behavior for a knot whose master complex has boxes and is not a torus knot.

3.5.2 Figure Eight

We first look at the master complex for 4_1, and then its quotients, as shown in Figure 3.8.

The invariants for 4_1 are

$$HFK_n(4_1) \cong \mathbb{Q} \oplus \mathbb{Q} \oplus \mathbb{Q} \oplus \mathbb{Q} \oplus \frac{\mathbb{Q}[U]}{(U^n)}$$

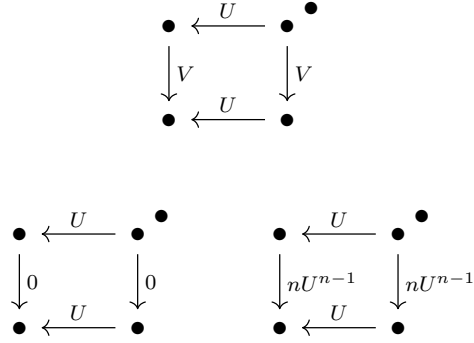$$HFK^-(4_1) \cong \mathbb{Q}[U] \oplus \mathbb{Q} \oplus \mathbb{Q}.$$

$$
\begin{array}{ccc}
\bullet & \xleftarrow{\;U\;} & \bullet\!\!\bullet \\
{\scriptstyle V}\big\downarrow & & \big\downarrow{\scriptstyle V} \\
\bullet & \xleftarrow{\;U\;} & \bullet
\end{array}
$$

$$
\begin{array}{ccc}
\bullet & \xleftarrow{\;U\;} & \bullet\!\!\bullet \\
{\scriptstyle 0}\big\downarrow & & \big\downarrow{\scriptstyle 0} \\
\bullet & \xleftarrow{\;U\;} & \bullet
\end{array}
\qquad
\begin{array}{ccc}
\bullet & \xleftarrow{\;U\;} & \bullet\!\!\bullet \\
{\scriptstyle nU^{n-1}}\big\downarrow & & \big\downarrow{\scriptstyle nU^{n-1}} \\
\bullet & \xleftarrow{\;U\;} & \bullet
\end{array}
$$

Figure 3.8 On the top: the complex $CFK_{U,V}(4_1)$, where each dot represents the module $\mathbb{Q}[U,V]$. On the left: the complex $CFK^-(4_1)$, where each dot represents the module $\mathbb{Q}[U]$. On the right: the complex $CFK_n(4_1)$, where each dot represents the module $\frac{\mathbb{Q}[U]}{(U^n)}$.

Again, the universal coefficient theorem gives us the following:

$$
HFK_n(4_1) \cong HFK^-(4_1) \underset{\mathbb{Q}[U]}{\otimes} \frac{\mathbb{Q}[U]}{(U^n)} \bigoplus \mathrm{Tor}_1^{\mathbb{Q}[U]}(HFK^-(4_1); \mathbb{Q}[U])
$$

$$
\cong \frac{\mathbb{Q}[U]}{(U^n)} \oplus \mathbb{Q} \oplus \mathbb{Q} \oplus \mathbb{Q} \oplus \mathbb{Q}.
$$

CHAPTER 4

DEEPLY SLICE KNOTS

This chapter is dedicated to work stemming from a collaborative project with three other doctoral candidates at Michigan State University: Rob McConkey, Christopher St. Clair, and Chen Zhang. Theorems will be labeled accordingly, and many figures were also collaborative efforts.

The primary conclusion of the project is the following result.

Theorem 4.0.1 (McConkey, St. Clair, W., Zhang). *For the first 6-crossing knot, $K = 6_1$, the Whitehead double of the dual knot to $1/n$ surgery along K, $D_+(\mu_{1/n}(K))$, is not slice in $S^3_{\frac{1}{n}}(K) \times I$ for $n \in \mathbb{Z}$, but is slice in a contractible 4-manifold with boundary $S^3_{1/n}(K)$.*

Our calculations motivate the following conjecture.

Conjecture 4.0.2. If a non-trivial knot K is slice in the 4-ball, then the Whitehead double of the dual knot to $1/n$ surgery along K, $D_+(\mu_{1/n}(K))$, is not slice in $S^3_{\frac{1}{n}}(K) \times I$ for $n \in \mathbb{Z}$, despite being slice in a contractible 4-manifold with boundary $S^3_{1/n}(K)$.

Conjecture 4.0.3. If a non-trivial knot K is slice in the 4-ball and has an acyclic summand in its knot Floer complex over $\mathbb{F}[U, V]/(UV)$ with a vertically and horizontally simplified basis, then the Whitehead double of the dual knot to $1/n$ surgery along K, $D_+(\mu_{1/n}(K))$, is not slice in $S^3_{\frac{1}{n}}(K) \times I$ for $n \in \mathbb{Z}$.

4.1 Topological Preliminaries

So far, little discussion on some of the most active topics in knot theory (and low-dimensional topology, for that matter) are present. We rectify that here, where we define the integral components to Theorem 4.0.1.

4.1.1 Satellite Knots

There is an operation on knots called *satellite operations*, where one constructs a new knot from two given knots. Given a knot P embedded in the solid torus $S^1 \times \mathbb{D}^2$ and K
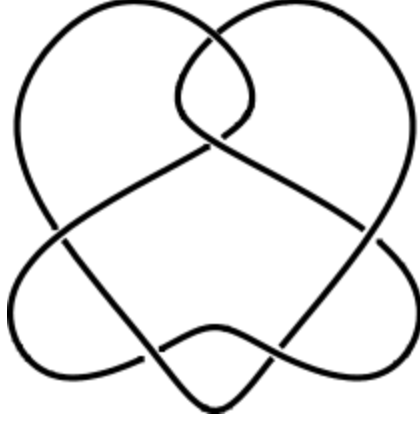
Figure 4.1 A common projection of the first 6-crossing knot, 6_1.

an arbitrary knot in S^3, gluing $S^1 \times \mathbb{D}^2$ along their common torus boundary to $S^3 \setminus \nu(K)$ yields a new knot in S^3, called the *satellite knot* $P(K)$, where the meridians of the tori are identified and the longitude of $S^1 \times \mathbb{D}^2$ is identified with the Seifert longitude of K. We call $P \subset S^1 \times \mathbb{D}^2$ the *pattern knot* and $K \subset S^3$ the *companion knot*.

The pattern appearing in Theorem 4.0.1 is the Whitehead pattern, denoted D_+. Here, the Whitehead pattern is the positively (hence the "+" in the symbol) clasped unknot wrapped around the S^1 factor of the solid torus in which its embedded. A figure involving the right handed trefoil as companion to the Whitehead pattern is shown in Figure 4.2.

4.1.2 Slice Knots

Given a smooth 4-manifold X whose boundary is Y, we say a knot $K \subset Y$ is *smoothly slice*, or simply *slice in X*, if there exists a smoothly embedded disc $\mathbb{D} \hookrightarrow X$ such that $K = \partial \mathbb{D} \subset \partial X = Y$. A schematic of a slice disc as well as a trivial example is shown in Figure 4.3. Sliceness is an extremely active topic for study when considering knots in S^3 thought of as the boundary of the standard smooth 4-ball, B^4. When not specified, when we say "K is slice," we mean that $K \subset S^3$ is slice in B^4. A particular knot invariant coming from knot Floer homology, the τ-invariant, is a concordance invariant, and hence can obstruct sliceness of a knot. We discuss this in further detail in Section 4.3.2. For a nice survey on knot concordance, see [Liv05].

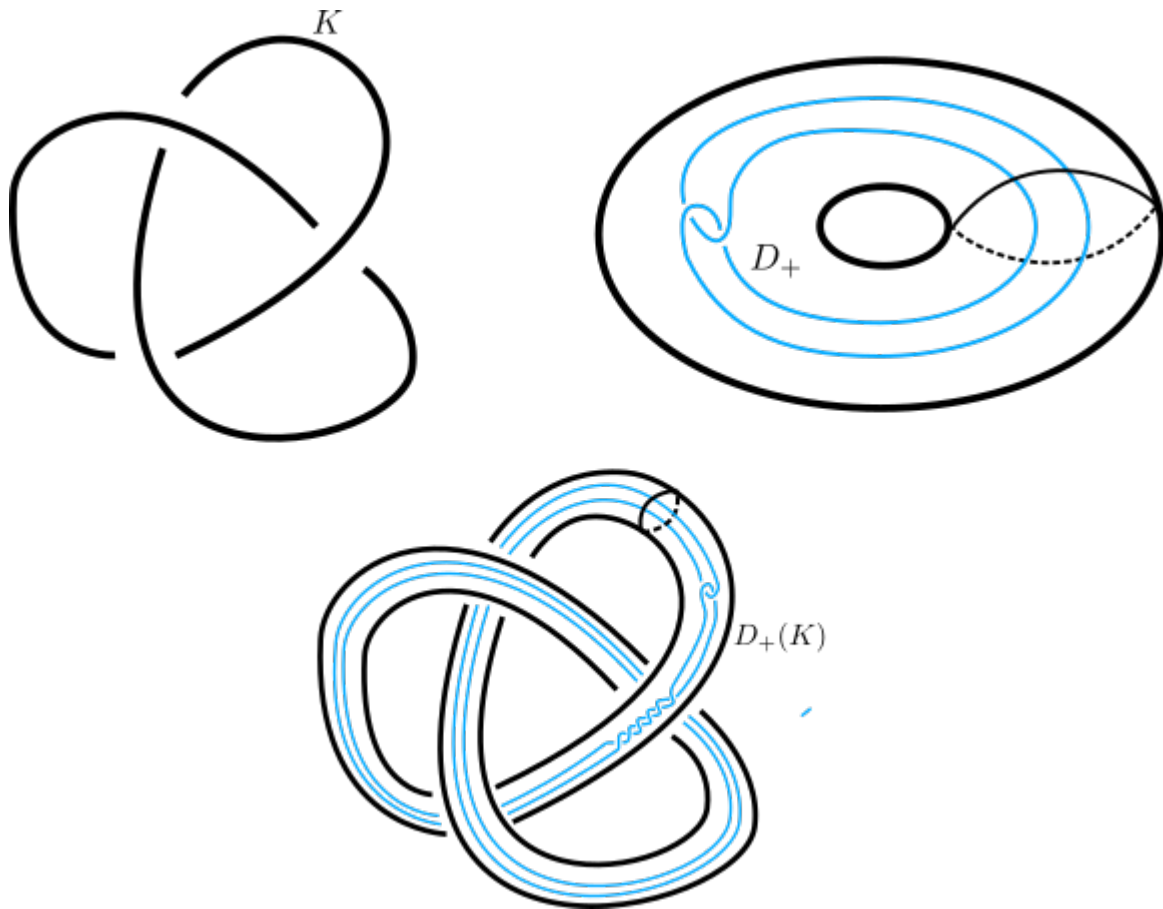Recall from Section 3.1.1 that surgery along K requires removing a solid torus in S^3 and

Figure 4.2 Left: A diagram for the right handed trefoil in S^3. Right: The Whitehead pattern, D_+, in $S^1 \times \mathbb{D}^2$. Bottom: A diagram for the knot $D_+(T_{2,3})$ in S^3.
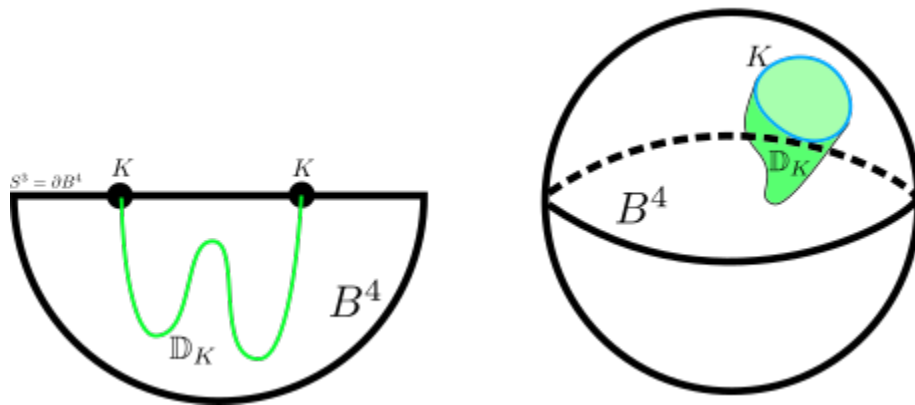

Figure 4.3 Left: A half-dimensional schematic of a slice disc for some knot K. Right: A slice disc schematic for the unknot, pushed into B^4.
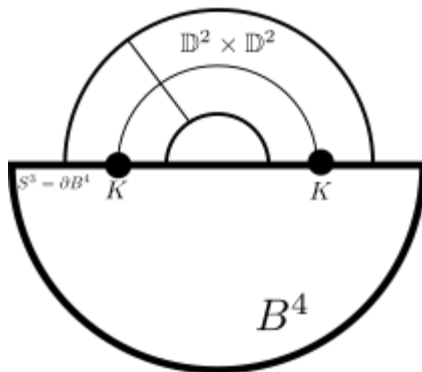
Figure 4.4 A half-dimensional schematic if a 2-handle attachment.

gluing it back in. The core of the surgery solid torus $S^1 \times \mathbb{D}^2$ once glued in to produce the surgered manifold is often called the *dual knot* to the surgery along K. In the case of $1/n$ surgery, we denote the dual knot as $\mu_{1/n}(K) \subset S^3_{1/n}(K)$. Much information is known about dual knots as well as various flavors of their knot Floer homology, including surgery formulae in [HHSZ22].

There is a feature of the dual knots that needs highlighting. Performing integral (that is, $p/q \in \mathbb{Z}$) surgery along a knot K in a 3-manifold Y corresponds to attaching 4-dimensional 2-handles, $\mathbb{D}^2 \times \mathbb{D}^2$, to the 4-manifold X whose boundary is Y (See Figure 4.4). Therefore, the core of the surgery torus is also the isotopic to the boundary of the cocore (the second $\mathbb{D}^2$ factor) of the attached 2-handle. Thus, the dual knot is slice in the 4-manifold $(Y \times I) \cup (2 - \text{handle})$, where the slice disc is the cocore of the 2-handle itself. For a reference on handle decompositions of 4-manifolds and Kirby calculus, see [GS99]. Moreover,

Theorem 4.1.1 ([Gor75]). *If K is slice, then there is a smooth, contractible 4-manifold W with boundary $S^3_{1/n}(K)$.*

There is a nice Kirby diagram for such a 4-manifold W obtained from the surgery diagram for $S^3_{1/n}(K)$, show in Figure 4.6. We first note that the dual knot to $1/n$ surgery along K looks like a pushoff of K in the surgery diagram in Figure 4.5. We then perform a Kirby move known as the *slam dunk* to obtain a surgery diagram with 0-framed surgery on K and
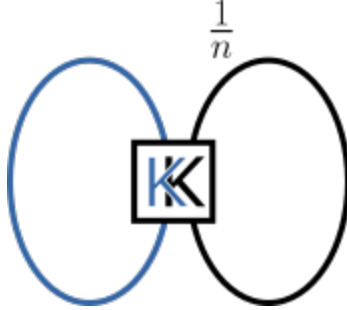
Figure 4.5 A surgery diagram for $1/n$ surgery along K, keeping track of the dual knot to the surgery, $\mu_{1/n}(K)$, in blue. Also, a Kirby diagram for a 4-manifold whose boundary is $S^3_{1/n}(K)$.
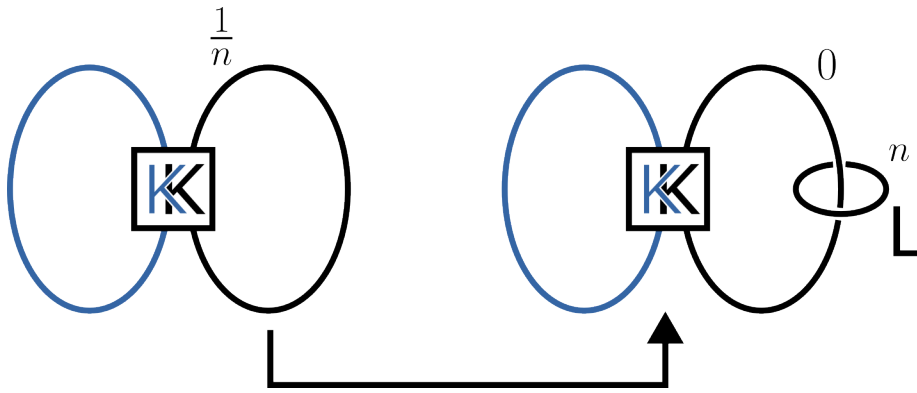

Figure 4.6 A *slam dunk* Kirby move applied to obtain a Kirby diagram for a new 4-manifold, W, whose boundary is homeomorphic to $S^3_{1/n}(K)$.

n-framed surgery on a new, unknotted component, denoted L. Finally, slide the dual knot representative over K itself to obtain the desired surgery diagram for $S^3_{1/n}(K)$. Now we show that all the Kirby diagrams in Figure 4.7 are Kirby diagrams for W, since each arrow only describes isotopies of the $\mu_{1/n}(K)$ in $S^3_{1/n}(K)$.

Proposition 4.1.2. *Suppose K is slice. Then the Kirby diagram on the right hand side of Figure 4.6 describes a smooth, contractible 4-manifold W whose boundary is $S^3_{1/n}(K)$.*

Proof. First, we note that the Kirby diagram is a surgery diagram for $S^3_{1/n}(K)$, by Kirby's Theorem [Kir78]. This is because we used only Kirby moves to manipulate the diagram, keeping track of the isotopy class of the dual knot, in red. Since K is slice in $S^3 = \partial B^4$, we begin by removing a neighborhood of a slice disc for K. This neighborhood is diffeomorphic
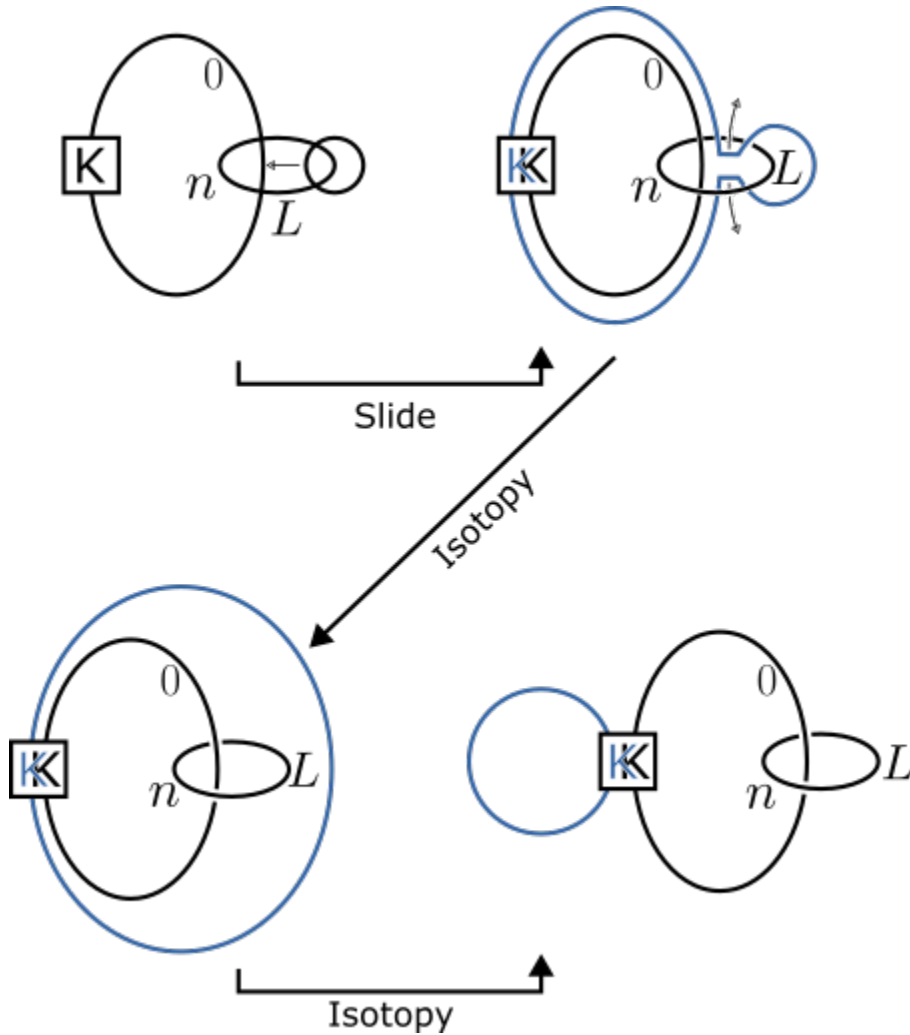
Figure 4.7 The process (in reverse) of obtaining a nice Kirby diagram for W, featured in the top left.

to $\mathbb{D}^2 \times \mathbb{D}^2$, with the first factor thought of as the slice disc, and the second as the thickening to a neighborhood. Hence, we are really removing a 2-handle from B^4 by introducing instead its canceling 1-handle, as in the "digging a ditch" analogy in [GS99]. With this perspective, we can see that the fundamental group of $B^4 \setminus (\mathbb{D}^2 \times \mathbb{D}^2)$ is generated by a meridian of the boundary of the removed disc; that is, a meridian of K. Now, we attach the other 2-handle with framing n along L, which is also a meridian of K, killing that generator in $\pi_1(B^4 \setminus (\mathbb{D}^2 \times \mathbb{D}^2))$, so $W = (B^4 \setminus (\mathbb{D}^2 \times \mathbb{D}^2)) \cup (2 - \text{handle})$ is contractible. $\qquad \square$

The particular feature of the dual knot to $1/n$ surgery of import is the following.

Lemma 4.1.3. *The dual knot to $1/n$ surgery along a slice knot $K \subset S^3$, $\mu_{1/n}(K) \subset S^3_{1/n}(K)$, is slice in W as in Theorem 4.1.1.*

Proof. This can readily be seen using the argument above, since the blue curve is the dual knot to n surgery on L in Figure 4.6. Thus, it is the boundary of the core of the 2-handle attached along L, which is a smooth disc in W. □

A well known fact about Whitehead doubling in S^3 is that the Whitehead double of a smoothly slice knot is again smoothly slice. Analogously, we achieve the following corollary:

Corollary 4.1.4. *The Whitehead double of the dual knot to $1/n$ surgery along a slice knot $K \subset S^3$, $D_+(\mu_{1/n}(K))$, is slice in W as in Theorem 4.1.1.*

Proof. By Lemma 4.1.3, the dual knot is itself slice. Given an annulus with one boundary component the dual knot and one boundary the unknot, guaranteed by sliceness, then we can "Whitehead double" the annulus in the same fashion as the dual knot itself. Since the Whitehead double of the unknot is again the unknot, we have presented an annulus between the Whitehead double of the dual knot and the unknot. □

In [KR21], the concept of *deeply slice* knots is introduced in a proposed strategy to answer a question on the Kirby list, attributed to Akbulut.

Definition 4.1.5 (Deeply Slice)**.** A knot $K \subset \partial X$ is *deeply slice* in X in X if it is slice in X but K is not slice in $\partial X \times I$.

That is to say that not only is the given slice disc not in $\partial X \times I$ but there is no slice disc there. In essence, this means that the slice disc is "interesting" because it requires use of the topology of the 4-manifold X rather than just what happens near the boundary. Then Akbulut's question in [Kir97] can be phrased as: Are there contractible, smooth 4-manifolds with boundary an integral homology 3-sphere which contain deeply slice knots that are null-homotopic in the boundary? With this definition, one can interpret Theorem 4.0.1 as saying that the Whitehead double of the dual knot is deeply slice in W described above. If the

generalization in Conjecture 4.0.2 holds, there would be a good place to look to find such knots.

4.2 Bordered Floer Theory

The first main tool used to obstruct the sliceness of the Whitehead double of the dual knot in a collar neighborhood of the boundary of W, i.e. $S^3_{1/n}(K) \times I$, is a version of Heegaard Floer homology associated to 3-manifolds with boundary, called *bordered Heegaard Floer homology*. The most consolidated resource on the matter is [LOT18]. Since then, bordered Heegaard Floer homology has led to significant results in 3-manifold topology and knot theory. In [HRW23, HRW22, Han23], Hanselman, Rasmussen, and Watson use the framework of bordered Heegaard Floer homology to construct a very useful description of knot Floer homology using *immersed curves*, which is the description we use here.

4.2.1 Immersed Heegaard Diagrams

As with the variants of Heegaard Floer theory discussed in Chapter 2, bordered theory also begins with a Heegaard diagram. *Immersed Heegaard diagrams* arise as a "composition" of two components, corresponding to *pairing theorems* in bordered Heegaard Floer homology. In this case, immersed Heegaard diagrams are built from pairing an immersed multicurve in a marked torus, thought of as the boundary of a bordered 3-manifold, and a pointed *bordered Heegaard diagram*. This definition and further discussion of immersed Heegaard Floer theory in full generality can also be found in [CH23].

Definition 4.2.1. An *immersed doubly-pointed Heegaard diagram* is a tuple $\mathcal{H} = (\Sigma_g, \boldsymbol{\alpha}, \boldsymbol{\beta}, w, z)$ where

- Σ_g is a closed oriented genus g surface,

- $\boldsymbol{\alpha} = \{\alpha_1, ..., \alpha_{g-1}, \boldsymbol{\alpha}_g\}$ is a collection of curves in Σ_g where $\{\alpha_1, ..., \alpha_{g-1}\}$ are embedded and disjoint, $\boldsymbol{\alpha}_g = \{\alpha_g^1, ..., \alpha_g^n\}$ is a collection of immersed curves decorated with local systems for which α_g^1 has the trivial local system, $\{\alpha_1, ..., \alpha_{g-1}, \alpha_g^1\}$ are linearly independent in $H_1(\Sigma_g; \mathbb{Z})$, and each α_g^i is trivial in $H_1(\Sigma_g; \mathbb{Z})/(\alpha_1, ..., \alpha_{g-1})$ for $i > 1$,

- $\boldsymbol{\beta} = \{\beta_1, ..., \beta_g\}$ is a collection of embedded disjoint curves in Σ_g which are linearly independent in $H_1(\Sigma_g; \mathbb{Z})$, and

- w and z are basepoints on Σ_g lying in the same component of $\Sigma_g \setminus \boldsymbol{\alpha}$ and in the same component of $\Sigma_g \setminus \boldsymbol{\beta}$.

Often times, and in this discussion, the local systems involved are all trivial. Also, we often denote $\boldsymbol{\alpha}_g$ by $\boldsymbol{\alpha}_{im}$ for "immersed alpha curves," following conventions in [CH23]. As usual, there are admissibility conditions on these kinds of Heegaard diagrams. We refer to [CH23] for details.

4.2.2   Knot Floer Complexes

We now discuss another way to get the knot Floer chain complex, now from an immersed Heegaard diagram.

Definition 4.2.2. Given an immersed doubly-pointed Heegaard diagram $\mathcal{H} = (\Sigma_g, \boldsymbol{\alpha}, \boldsymbol{\beta}, w, z)$, the *"UV equals zero" knot Floer complex* of $\mathcal{H}$ is freely generated over $\mathcal{R} = \mathbb{F}[U, V]/(UV)$ by all intersection points $\mathbf{x} \in \mathbb{T}_\alpha \cap \mathbb{T}_\beta$, denoted

$$CFK_{\mathcal{R}}(\mathcal{H}) := \bigoplus_{\mathbf{x} \in \mathbb{T}_\alpha \cap \mathbb{T}_\beta} \mathcal{R}\langle \mathbf{x} \rangle,$$

with boundary map defined on generators by

$$\partial_{\mathcal{R}}(\mathbf{x}) := \sum_{\substack{y \in \mathbb{T}_\alpha \cap \mathbb{T}_\beta}} \sum_{\substack{\phi \in \pi_2(x,y) \\ \mu(\phi)=1}} \#\widehat{\mathcal{M}}(\phi) U^{n_w(\phi)} V^{n_z(\phi)} \mathbf{y}.$$

Working over the ring $\mathcal{R} = \mathbb{F}[U, V]/(UV)$, often called the "UV equals zero" ring, has become increasingly popular in studying knot Floer homology, and is useful in eliminating pesky arrows in the chain complex. As is the case for the full knot Floer complex in Section 2.2.2, $CFK_{\mathcal{R}}(\mathcal{H})$ supports a bigrading by $(\mathrm{gr}_U, \mathrm{gr}_V)$ or by (gr_U, A) defined the same way. As is obligatory, the following theorems guarantee an invariant chain complex.

Theorem 4.2.3 ([CH23]). *The complex $(CFK_{\mathcal{R}}(\mathcal{H}), \partial_{\mathcal{R}})$ is a chain complex, i.e. $\partial_{\mathcal{R}}^2 = 0$.*

Theorem 4.2.4 ([CH23]). *The bigraded chain homotopy type of $(CFK_{\mathcal{R}}(\mathcal{H}), \partial_{\mathcal{R}})$ is invariant under isotopies of the $\boldsymbol{\alpha}$ curves and $\boldsymbol{\beta}$ curves, handeslides, and (de)stabilization of the Heegaard diagram, $\mathcal{H}$.*

Later, in the discussion of pairing theorems, we will see that this complex is chain homotopy equivalent to the full knot Floer complex of the compatible knot with the identification $UV = 0$ in the ground ring. To see the relationship between a knot-3-manifold pair and the knot Floer complex, we turn our attention to the two pieces paired to create an immersed Heegaard diagram.

4.2.3 Doubly-pointed Bordered Heegaard Diagrams

A doubly-pointed bordered Heegaard diagram for a pair (Y, K) is to a *bordered Heegaard diagram* for Y as a doubly-pointed Heegaard diagram for a pair (Y, K) is to a Heegaard diagram for Y. That is, we first start with the following information which encodes a *bordered 3-manifold* $(Y, \mathcal{Z}, \phi)$, where $\mathcal{Z}$ and ϕ are some auxiliary data specifying a parametrization of the boundary of Y.

Definition 4.2.5 (Bordered Heegaard Diagram). A *bordered Heegaard diagram* for a smooth 3-manifold Y with boundary is a tuple $(\overline{\Sigma}_g, \boldsymbol{\alpha}, \boldsymbol{\beta}, w)$ where

- $\overline{\Sigma}_g$ is a genus g surface with a single boundary component,

- $\boldsymbol{\beta}$ is a collection of g pairwise disjoint properly embedded simple closed curves in the interior of $\overline{\Sigma}_g$ which are linearly independent in $H_1(\overline{\Sigma}_g; \mathbb{Z})$,

- $\boldsymbol{\alpha}$ is a collection of $g - k$ pairwise properly disjoint embedded simple closed curves $\boldsymbol{\alpha}^c := \{\alpha_1^c, ..., \alpha_{g-k}^c\}$ in the interior of $\overline{\Sigma}_g$ and $2k$ pairwise disjoint properly embedded arcs $\boldsymbol{\alpha}^a := \{\alpha_1^a, ..., \alpha_{2k}^a\}$ in $\overline{\Sigma}_g$ with transverse intersection with $\partial\overline{\Sigma}_g$, and

- w is a point on $\partial\overline{\Sigma}_g \setminus (\boldsymbol{\alpha} \cap \partial\overline{\Sigma}_g)$.

Given a bordered Heegaard diagram, reconstruction of the bordered 3-manifold is very similar to that of an ordinary Heegaard diagram. We outline the notable difference here.

Since there are now arcs $\boldsymbol{\alpha}^a$ in the diagram, we must complete them to circles to attach handles along them. Roughly speaking, this is done using the data of a *point matched circle* that encodes the parametrization of the boundary of the bordered 3-manifold. For further details, see [LOT18].

As we have come to expect, we have the following theorem.

Theorem 4.2.6 ([LOT18]). *Any bordered 3-manifold can be represented by some bordered Heegaard diagram.*

To complete the analogy, we now incorporate the information of a knot present in a bordered manifold.

Definition 4.2.7 (Doubly-pointed bordered Heegaard diagram). A *doubly-pointed bordered Heegaard diagram* for Y compatible with a knot $K \hookrightarrow Y$ is a tuple $(\overline{\Sigma}_g, \boldsymbol{\alpha}, \boldsymbol{\beta}, w, z)$ where

- $(\overline{\Sigma}_g, \boldsymbol{\alpha}, \boldsymbol{\beta}, w)$ is a bordered Heegaard diagram for Y as in Definition 4.2.5 and

- z is a basepoint along with w in $\overline{\Sigma}_g \setminus (\alpha^c \cup \boldsymbol{\beta})$ such that K can be recovered from w and z.

The recovery of the knot is exactly the same as it is for Definition 2.2.1. As usual, every knot in a bordered 3-manifold can be realized by a doubly-pointed bordered Heegaard diagram. These diagrams are the first pieces in constructing an immersed Heegaard diagram.

4.2.4 Immersed Curves

The second ingredient in an immersed Heegaard diagram is the *immersed multicurve* in the marked boundary of a knot compliment, the *marked torus*. The marked torus is simply the standard torus, thought of as $\mathbb{R}^2/\mathbb{Z}^2$ in the plane, where the x-axis is the *preferred longitude* and the y-axis is the *preferred meridian*, and a basepoint z located at $(1 - \epsilon, 1 - \epsilon)$ for as small $\epsilon > 0$ as we like. An *immersed multicurve* is a set of immersed curves in the marked torus away from z decorated with *local systems*, which we suppress, since our result

does not concern them directly. We often simply say *immersed curve* to mean an immersed multicurve.

Immersed curves conveniently package the information of $CFK^-(Y, K)$ in the form of the *bordered invariant*, sometimes denoted $\widehat{HF}(Y \setminus \nu(K))$, which is an invariant of a bordered 3-manifold arising from a bordered Heegaard diagram. For discussions on the immersed curve formulation of bordered Heegaard Floer homology, see [HRW23], [HRW22], and [Han23]. Technically, to carry out this packaging, a particular basis is required for $CFK^-(Y, K)$. Recalling that $CFK^-(Y, K)$ comes with two filtrations, one by the action of multiplying by U and the other by the Alexander filtration, as in [HRW22], we may choose a representative of the chain homotopy type of $CFK^-(Y, K)$ for which the boundary map ∂^- strictly decreases one of these filtrations. A *filtered basis* for $CFK^-(K)$ is $\{v_i\}$ such that the equivalence classes $\{[v_i]\}$ in the associated graded complex $gCFK^-(Y, K) = \bigoplus \mathcal{F}_{A(x)}/\mathcal{F}_{A(x)-1}$ are a basis.

Definition 4.2.8 ([HRW22])**.** A filtered basis $\{v_i\}$ is *vertically simplified* if for each v_i, either $\partial v_i \in U \cdot CFK^-(K)$ or $\partial v_i \sim v_j + x$ where $x \in U \cdot CFK^-(K)$. The filtered basis is *horizontally simplified* if for each v_i with Alexander filtration level $A(v_i) = l$, either $A(\partial v_i) < l$ or $A(\partial v_i) = U^k v_j + x$ where $A(U^k v_j) = l$ and $A(x) < l$.

Being vertically simplified can be thought of as requiring that each basis generator only has one vertical arrow pointing to or away from it, and likewise for horizontally simplified. The complex in Figure 2.8 is both vertically and horizontally simplified. For any knot, $CFK^-(Y, K)$ always admits a vertically simplified basis and always admits a horizontally simplified basis. As a warning, it may not be the case that $CFK^-(Y, K)$ admits a basis which is simultaneously vertically and horizontally simplified. Nevertheless, we restrict our attention to when there is a basis which is both.

We now describe an algorithm for obtaining an immersed curve from $CFK^-(Y, K)$, following the method in [HRW22]. It is most convenient to present this curve as a lift in the cover of the marked torus, $[-1/2, 1/2] \times \mathbb{R}$, where the interval corresponds to the preferred longitude λ and $\{-1/2\} \times \mathbb{R}$ and $\{1/2\} \times \mathbb{R}$ are identified and is a lift of the preferred

meridian, μ. We then center the lifts of the basepoint z at $\{0\} \times \{n + 1/2\}$ for $n \in \mathbb{Z}$. This setup, along with a curve obtained from the following procedure, can be seen in Figure 4.8.

Proposition 4.2.9 ([HRW22])**.** *Given a horizontally and vertically simplified basis for $CFK^-(K)$, a lift of the immersed multicurve $\boldsymbol{\alpha}_{im} = \widehat{HF}(Y \setminus \nu(K))$ in the infinite strip can be obtained by the following procedure:*

1. *For each basis element v_i of $CFK^-(K)$, place a short horizontal segment at $[-1/4, 1/4] \times \{t\}$ where $t = A(v_i)$.*

2. *If $CFK^-(K)$ contains a vertical arrow from v_i to v_j, then connect the* left *endpoints of the horizontal segments corresponding to v_i and v_j by a vertical arc.*

3. *If $CFK^-(K)$ contains a horizontal arrow from v_i to v_j, then connect the* right *endpoints of the horizontal segments corresponding to v_i and v_j by a vertical arc.*

4. *Connect the unique horizontal segment with an unattached left endpoint to $\{-1/2\} \times \{0\}$ and the unique horizontal line segment with an unattached right endpoint to $\{1/2\} \times \{0\}$ each with an arc.*

4.2.5 Pairing Theorems

Ordinarily, bordered Heegaard Floer homology is presented using type D modules and type A modules over differential graded algebras associated to the boundaries of the manifolds involved. Then a special model of the derived tensor product, the *box tensor product*, is used to obtain a representative of the chain homotopy class of the Heegaard Floer complex or knot Floer complex from Section 2.1. The genius and beauty of the immersed curves perspective is that we can now package all of the complicated algebraic information into pictures of curves. Many important invariants can then be read directly from the immersed Heegaard diagrams coming from pairing immersed curves with bordered Heegaard diagrams.

From a doubly-pointed bordered Heegaard diagram $\mathcal{H}$ as in Definition 4.2.5 and an immersed curve $\boldsymbol{\alpha}_{im}$ as described in Section 4.2.4, there is a way to pair them by gluing to
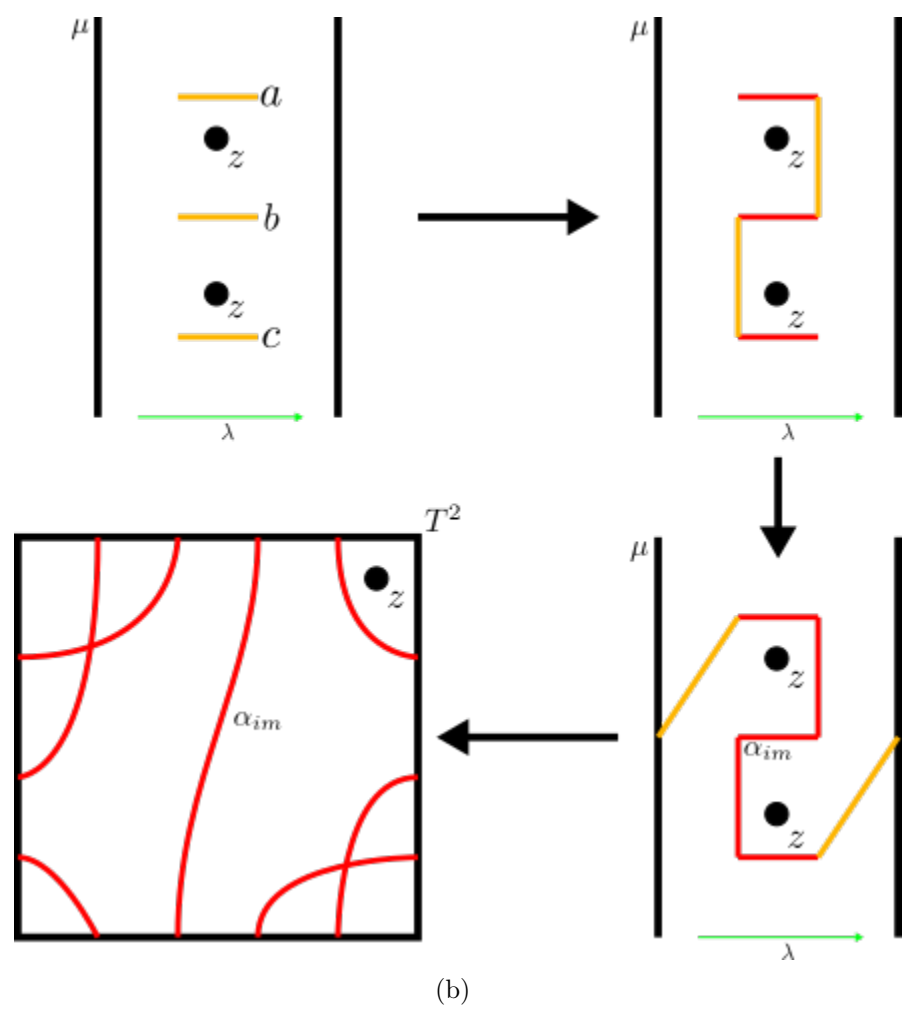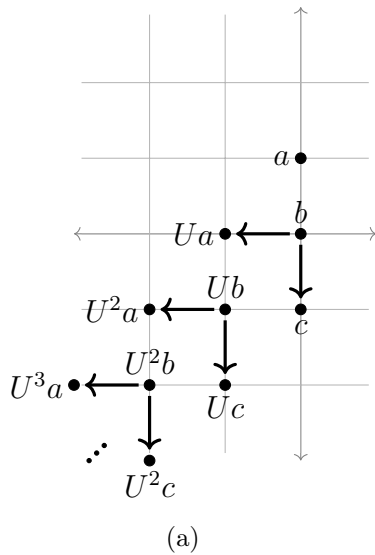
46

Figure 4.8 (a) $CFK^-(T_{2,3})$. (b) Each step of the construction in Proposition 4.2.9, with a projection to the marked torus on the bottom left.

obtain a doubly-pointed immersed Heegaard diagram $\mathcal{H}(\boldsymbol{\alpha}_{im})$ as in Definition 4.2.1. While a more detailed description can be found in [CH23], essentially, the two diagrams are glued along their common boundary, thought of as "filling in" the bordered Heegaard diagram with the immersed curve. After some isotopies, the resulting doubly-pointed immersed Heegaard diagram looks like a superposition of the bordered Heegaard diagram and the immersed curve. Figure 4.9 illustrates this process. One can remove many immersed points by looking at the curves in various lifts of the torus, such as the infinite strip. To see why this is useful, it is best to introduce the necessary pairing theorem, as it is one of the primary theorems applied to prove Theorem 4.0.1.

Theorem 4.2.10 ([CH23]). *Let $\mathcal{H}$ be a doubly-pointed bordered Heegaard diagram for a pattern knot $P \subset S^1 \times \mathbb{D}^2$, and let $\boldsymbol{\alpha}_K$ be the immersed multicurve associated to a companion knot K. Let $\mathcal{H}(\boldsymbol{\alpha}_K)$ be the immersed doubly-pointed Heegaard diagram obtained by pairing $\mathcal{H}$ with $\boldsymbol{\alpha}_K$. Then the $CFK_{\mathcal{R}}(\mathcal{H}(\boldsymbol{\alpha}_K))$ is bigraded chain homotopy equivalent to the knot Floer complex of the satellite knot $P(K)$ over $\mathcal{R}$, where $\mathcal{R} = \mathbb{F}[U, V]/(UV)$.*

Theorem 4.2.10 is actually a generalization of an earlier theorem of Chen in [Che23], presented below. In [CH23], they remark that Theorem 4.2.10 is particularly useful when the pattern knot is a *(1,1) pattern*, which means that it has a genus 1 doubly-pointed bordered Heegaard diagram. This is because the resulting immersed Heegaard diagram is also genus 1, so it is easy to extract $CFK_{\mathcal{R}}(\mathcal{H}(\boldsymbol{\alpha}_{im}))$ even when the curves self-intersect. In fact, the process is entirely combinatorial. We will see a classic example in Section 4.4. The earlier theorem, while less general, is still useful to present here as its proof more carefully specifies the homeomorphism of the pairing of the knot compliment and the pattern torus:

Theorem 4.2.11 ([Che23]). *Let $P \subset S^1 \times \mathbb{D}^2$ be a $(1, 1)$-pattern knot and K in S^3 a companion. Let $\boldsymbol{\alpha}_K \subset \partial S^3 \setminus \nu(K)$ be the immersed curve for K, and let $\mathcal{H}$ be a genus 1 bordered Heegaard diagram for P, thought of as curves and basepoints in $\partial S^1 \times \mathbb{D}^2$. Let $h : \partial(S^3 \setminus \nu(K)) \to \partial(S^1 \times \mathbb{D}^2)$ be an orientation preserving homeomorphism such that*
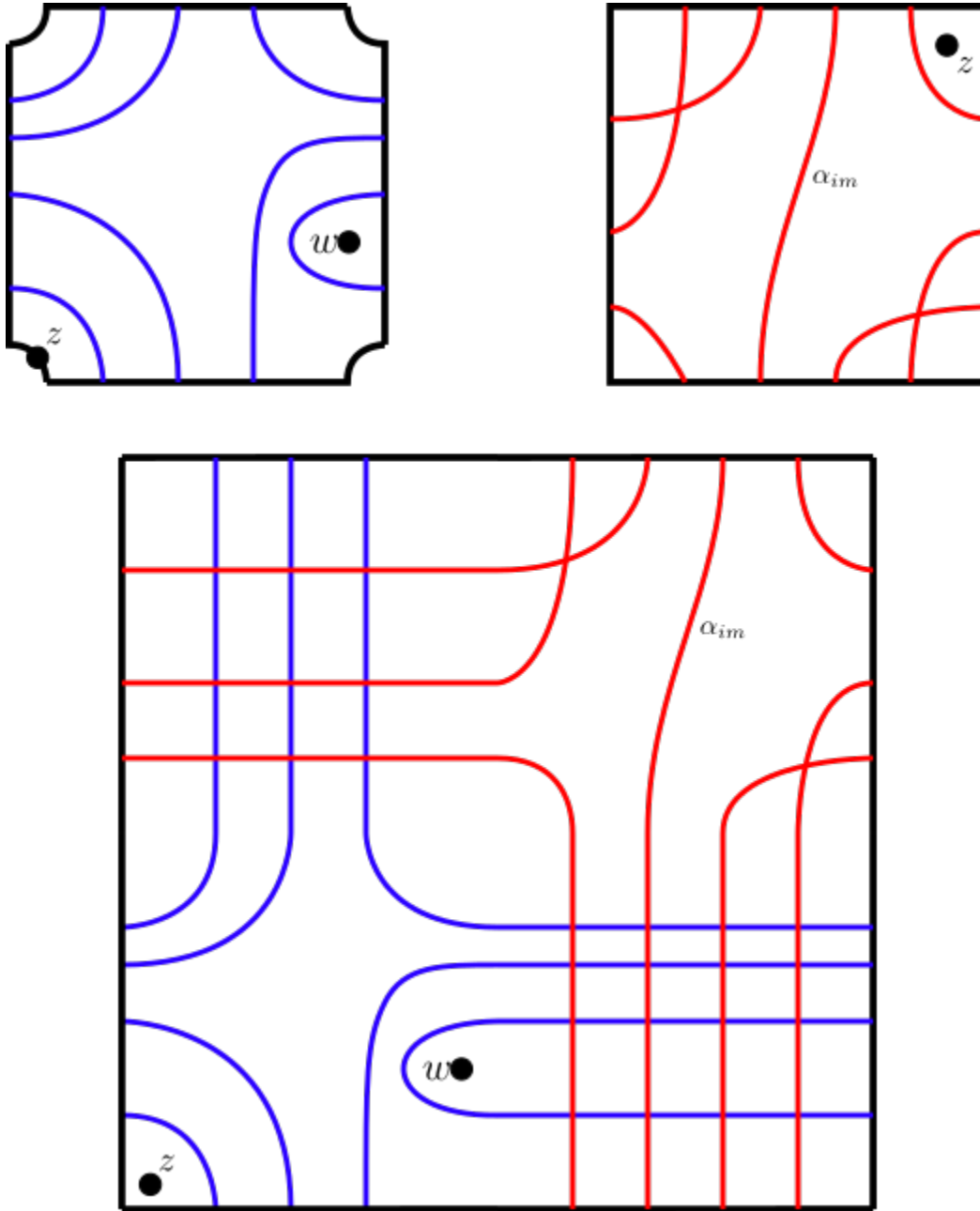
Figure 4.9 Top left: A bordered Heegaard diagram. Top right: An immersed curve in the marked torus. Bottom: The immersed Heegaard diagram obtained by gluing.

- h identifies the meridian and Seifert longitude of K with μ and λ respectively;

- h maps the z basepoint for $\boldsymbol{\alpha}_K$ to the z basepoint for $\mathcal{H}$;

- there is a regular neighborhood $U \subset \partial(S^1 \times \mathbb{D}^2)$ of z such that $U \cap (\lambda \cup \mu) = \emptyset$ and $U \cup h(\boldsymbol{\alpha}_K) = \emptyset$.

Suppose $\boldsymbol{\alpha}_K$ is connected. Then there is a grading-preserving isomorphism of chain complexes

$$\widehat{CFK}(\mathcal{H}(\boldsymbol{\alpha}_K)) \cong \widehat{CFK}(S^3, P(K)).$$

The goal is to adapt this theorem to manifolds other than S^3, and extend the chain homotopy equivalence to the $UV = 0$ complex $CFK_\mathcal{R}$ rather than simply $\widehat{CFK}$.

Theorem 4.2.12. *Let $\mathcal{H}$ be a doubly-pointed bordered Heegaard diagram for a pattern knot $P \subset S^1 \times \mathbb{D}^2$, and let $\boldsymbol{\alpha}_K$ be the immersed multicurve associated to a companion knot K. Let $\mathcal{H}(\boldsymbol{\alpha}_K)$ be the immersed doubly-pointed Heegaard diagram obtained by pairing $\mathcal{H}$ with $\boldsymbol{\alpha}_K$ using a framing change in accordance with $1/n$ surgery on K. Then the knot Floer complex $CFK_\mathcal{R}(\mathcal{H}(\boldsymbol{\alpha}_K))$ is bigraded chain homotopy equivalent to the knot Floer complex of the satellite knot $P(\mu_{1/n}(K))$ in $S^3_{1/n}(K)$ over $\mathcal{R}$, where $\mathcal{R} = \mathbb{F}[U,V]/(UV)$.*

Proof. The proof of Theorem 4.2.10 passes through an *arced bordered Heegaard diagram*, which is a version of a bordered Heegaard diagram for a manifold with two boundary components. The manifold in question is $S^1 \times \mathbb{D}^2 \setminus \nu(P)$, the compliment of the pattern knot in the solid torus. In their proof, the parametrization of the outer boundary is the usual meridian-longitude parametrization and the inner boundary is parametrized by the meridian of P and a longitude of P. Here, we will parametrize the outer boundary instead with a framing change given by the $1/n$ surgery we will perform along K. That is, a homeomorphism $\Phi_n : \partial_{\text{outer}}\big((S^1 \times \mathbb{D}^2) \setminus \nu(P)\big) \to \partial(S^3 \setminus \nu(K))$, given by how it acts on homology,

$$\Phi_n^* = \begin{bmatrix} 1 & 0 \\ n & -1 \end{bmatrix}.$$

50

Now, when pairing $\mathcal{H}$ with $\boldsymbol{\alpha}_K$, we simply take this map into account by adding Dehn twists in the torus for $\mathcal{H}$ to skew the diagram to slope $-1/n$ (really, we can skew either diagram using Dehn twists, but we prefer to look at covering spaces which maintain the basis already in place for $\boldsymbol{\alpha}_K$ rather than $\mathcal{H} = (\overline{\Sigma}_g, \boldsymbol{\alpha}, \boldsymbol{\beta}, w, z)$, so the linear map on $H_1(\overline{\Sigma}_g) = <\mu, \lambda>$ is the inverse of Φ_n^*). The remainder of the proof is unchanged from that of Theorem 4.2.10. $\square$

4.3 Invariants

All of the aforementioned diagrams grant access to a slew of numerical knot invariants, especially *concordance invariants*. While we forgo details on concordance and omit definitions of the invariants not involved in the proof of Theorem 4.0.1, we mention their existence.

4.3.1 Knot genus, τ, and ϵ

Given an immersed curve $\boldsymbol{\alpha}_K$ representing the bordered invariant of $S^3 \setminus \nu(K)$, the construction in Proposition 4.2.9 makes it easy to see two popular numerical invariants of K. To do this, it is easiest (while not required) to pull the immersed curve tight, to create a so-called *pegboard diagram*. For a knot, the immersed curve pulled tight will just be a vertical strand in the neighborhood of $\{0\} \times \mathbb{R}$, where the "pegs" are located, and one homologically horizontal strand which wraps around the infinite strip.

The genus of the knot, $g(K)$, is simply the difference between the maximum height achieved by $\boldsymbol{\alpha}_K$ and the minimum height achieved, rounded to the nearest integer when pulled tight. This is the same as checking how many pegs are encompassed by the curve and dividing by 2. The tau invariant of Ozsváth and Szabó, $\tau(K)$, can be see by starting anywhere on the horizontal strand and tracing to the right (in the positive interval direction) until hitting the vertical strand. The nearest integer height where they meet is $\tau(K)$. Finally, $\epsilon(K)$, defined by Hom, is shown by the behavior of the horizontal line segment after crossing the vertical portion. If the curve has an upward slope, $\epsilon(K) = 1$. If downward, $\epsilon(K) = -1$. If it continues straight, which is only possible if $\tau(K) = 0$ by Proposition 4.2.9, then $\epsilon(K) = 0$ as well.

For example, the curve for the right handed trefoil shown in Figure 4.8 has the following invariants: $\tau(T_{2,3}) = 1$, since the horizontal curve first intersects above the higher basepoint when traveling to the right (along the green arrow indicating λ). Then, since when leaving the vertical strand, the curve again has positive slope, μ, $\epsilon(T_{2,3}) = 1$ as well.

4.3.2 $\tau_\alpha(Y, K)$

From an immersed Heegaard diagram of genus 1, Chen gives a nice calculus for determining $\tau(K)$ along with the Alexander gradings of other generators in [Che23]. The calculus introduces to the diagram *A-buoys* attached to the $\boldsymbol{\beta}$ curves. Essentially, these A-buoys are small arrows which record the change in Alexander filtration level between two generators as we isotope away discs only crossing the z basepoint. Isotoping discs away is akin to canceling components of the differential on the filtered complex. The difference in Alexander filtration level between two intersection points indicates the lengths of differentials that we cancel, which corresponds to "turning the page" on the spectral sequence converging to the Heegaard Floer homology of the underlying 3-manifold, as described in Section **??**.

So, in practice, we perform isotopies to cancel differentials of filtration length one until we no longer can, recording the filtration change using A-buoys. We can then iterate this process for length two, or three, should we like, to see further pages in the spectral sequence. For a knot in S^3, there will eventually be only one remaining intersection point, whose Alexander grading is $\tau(K)$. However, for a knot in a 3-manifold other than S^3, such as a 3-manifold obtained by surgery, more than one intersection point may remain, since the 3-manifold might have $\mathrm{rk}\widehat{HF}(Y) > 1$.

In [HR23], Hedden and Raoux introduce the invariants $\tau_\alpha(Y, K)$, which are assignments to each Heegaard Floer homology class $\alpha \in \widehat{HF}(Y)$ and knot $K \subset Y$ a number which records the Alexander filtration level of α. Algebraically, $\tau_\alpha(Y, K)$ is the Alexander grading of the surviving generator of $\widehat{CFK}(Y, K)$ in the spectral sequence to $\widehat{HF}(Y)$. Geometrically, $\tau_\alpha(Y, K)$ gives a lower bound for the genus of surfaces with boundary K in 4-manifolds with boundary. The theorem is as follows.

Proposition 4.3.1 ([HR23]). *Let K be a null-homologous knot in Y. If $\Sigma \subset Y \times I$ is a smoothly embedded oriented surface with boundary $K \subset Y \times \{1\}$, then*

$$\tau_\alpha(Y, K) \leq g(\Sigma).$$

Corollary 4.3.2. *If $K \subset Y$ is slice in $Y \times I$, then $\tau_\alpha(Y, K) = 0$ for all $\alpha \in \widehat{HF}(Y)$.*

Proof. Recall that if K is slice, then it bounds a smooth disc in $Y \times I$. Equivalently, it means that K cobounds a smooth annulus with the unknot. If there exists some $\alpha \in \widehat{HF}(Y)$ with $\tau_\alpha(K) \neq 0$, Proposition 4.3.1 implies that the genus of any such surface is nonzero, a contradiction. $\square$

Clearly, this is a generalization of an already well known fact that the τ-invariant obstructs sliceness in B^4. Corollary 4.3.2 also implies that we can see obstructions to sliceness in immersed Heegaard diagrams of genus 1 using Chen's A-buoy calculus. In fact, the same way one detects the τ-invariant for the knot using A-buoys, one can detect the other $\tau_\alpha(Y, K)$ by checking the Alexander gradings of any surviving generators in the spectral sequence from knot Floer homology to $\widehat{HF}(Y)$ (yielded by considering the filtration induced by the presence of a knot). In Figure 4.12, the satellite knot still lives in S^3, which has a unique Spin^c structure, and thus only one τ_α, which is just the usual τ-invariant for the satellite knot. we treat an extended example in the next subsection.

4.4 Examples

Now that the meat of the theory is introduced, we move to illuminating examples. We turn our attention to the $(1,1)$ pattern knot of focus, the Whitehead double, D_+, depicted in Figure 4.2. A doubly-pointed bordered Heegaard diagram for D_+, denoted simply by $\mathcal{H}$ in this section, can be seen in Figure 4.10.

4.4.1 $D_+(T_{2,3})$

Now, we have a plethora of immersed curves with which we can check consistency with what we already know of knot Floer homology of satellites. We begin with the right handed
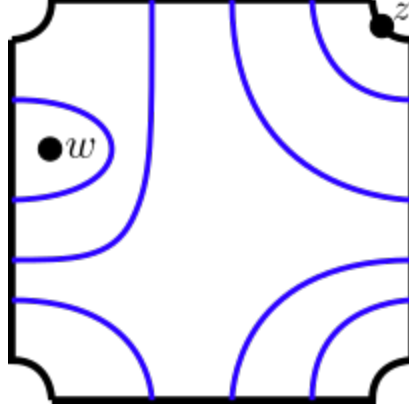
Figure 4.10 A genus 1 Heegaard diagram for the Whitehead pattern, D_+. We think of the two arcs $\{\alpha_1^a, \alpha_2^a\}$ as μ and λ, the two sides of $\overline{\Sigma}_g$, the punctured torus ($g = 1$). They intersect $\partial\overline{\Sigma}_g$ as required.
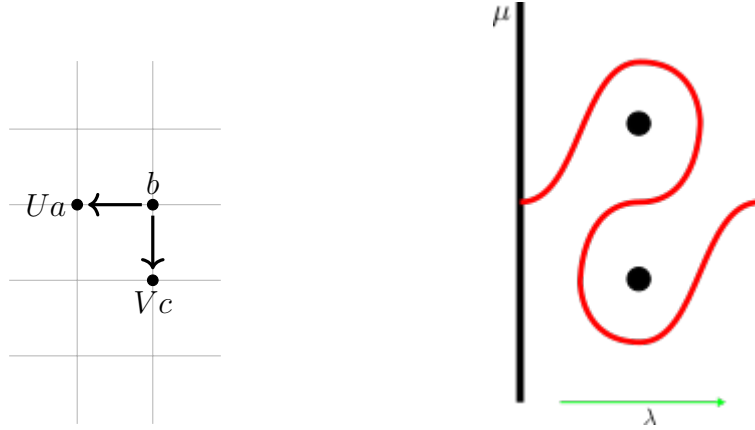

Figure 4.11 Left: A shorthand representation of the complex $CFK_{\mathcal{R}}(T_{2,3})$, the right handed trefoil. Right: The immersed curve arising from the complex on the left.

trefoil, since it is a torus knot. Its knot Floer complex over $\mathcal{R}$ is in Figure 2.8, which, for simplicity, we often draw only one copy, as in Figure 4.11. Following the procedure in Proposition 4.2.9, we obtain the immersed curve for the trefoil shown also in Figure 4.11.

From Figure 4.11, we see that $\tau(T_{2,3}) = 1$ and $\epsilon(T_{2,3}) = 1$. To establish $\tau(D_+(T_{2,3}))$, we pass to an immersed Heegaard diagram by paring $\boldsymbol{\alpha}_{T_{2,3}}$ and $\mathcal{H}$, as in Figure 4.12. To determine $\tau(D_+(T_{2,3}))$ from this immersed Heegaard diagram, we employ two steps. First, the Alexander grading of each intersection point in the diagram can be determined by looking at their relative Alexander gradings given by Whitney discs between them. Second, we
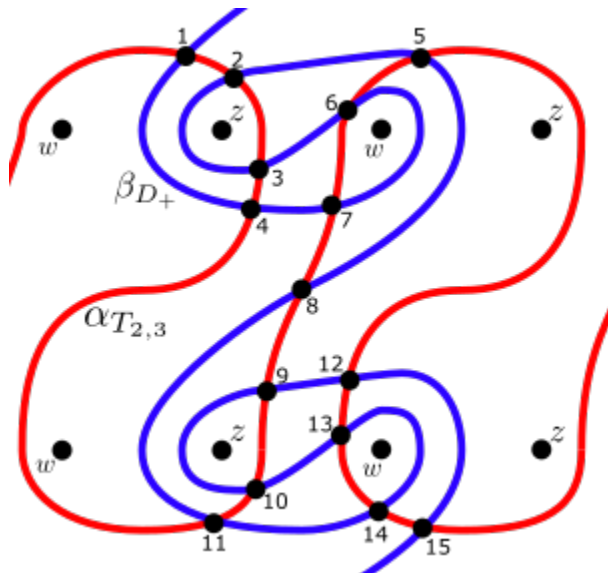
Figure 4.12 A lift of an immersed Heegaard diagram for the Whitehead double of the right handed trefoil in S^3.

symmetrize the gradings so that the top-most and bottom-most are just opposite in sign. This establishes the absolute Alexander grading of each generator of $CFK_{\mathcal{R}}(D_+(T_{2,3}))$ in this diagram. The gradings are as follows:

$\mathbf{x}$	$A(\mathbf{x})$
$4, 7, 11, 14$	1
$1, 3, 6, 8, 10, 13, 15$	0
$2, 5, 9, 12$	-1

Following Chen's A-buoy calculus, we begin canceling differentials of length one, then length two, and so on, until a single generator remains, corresponding to the single generator of $\widehat{HF}(S^3)$. Then $\tau(D_+(T_{2,3}))$ is the Alexander grading of the remaining generator, . The entire manipulation of the immersed Heegaard diagram is carried out in Figures 4.13 and 4.14. We see that the only generator surviving after pulling $\boldsymbol{\beta}$ straight is x_7, which has $A(x_7) = 1$. Thus, the singular τ_α corresponding to the only generator $\alpha \in \widehat{HF}(S^3)$ is just $\tau(D_+(T_{2,3})) = 1$. Consequently, $D_+(T_{2,3})$ is not slice in S^3.
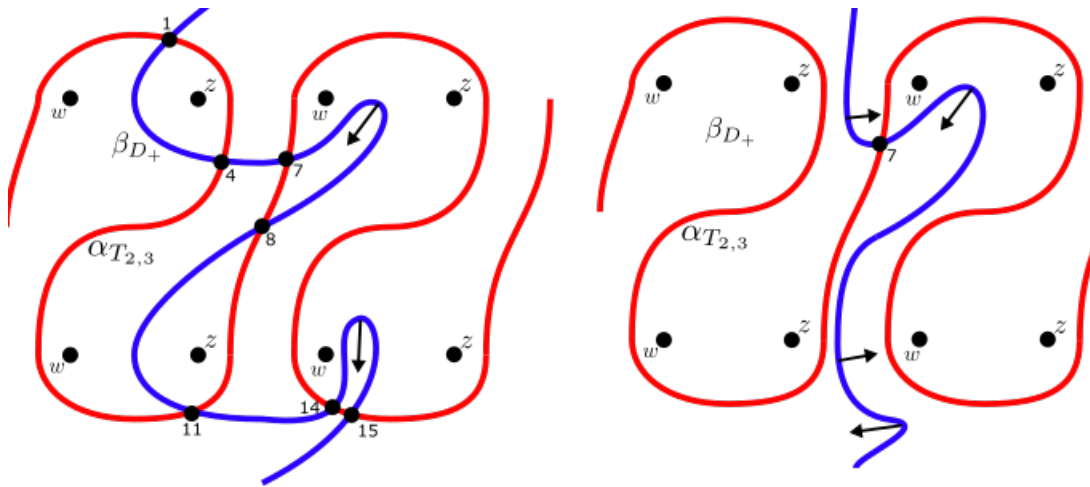
Figure 4.13 Cancellation of length one differentials. β_{d_+} is essentially pulled tight across the z basepoints.
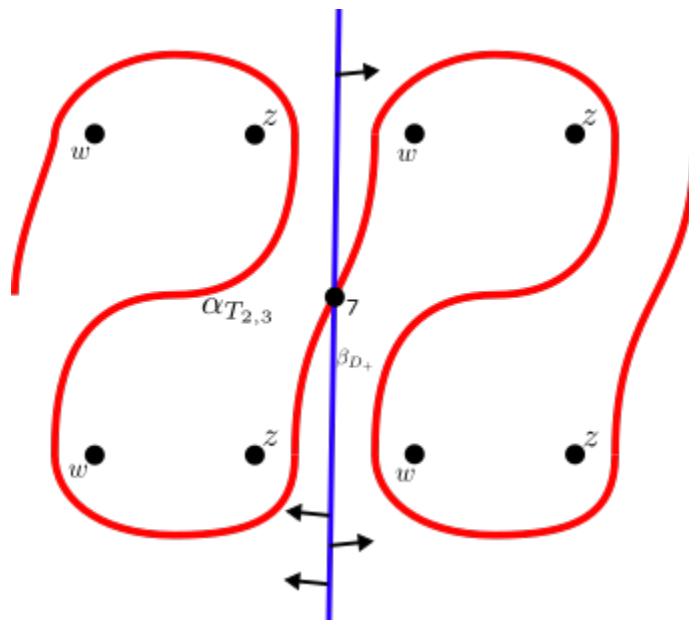

Figure 4.14 The immersed Heegaard diagram for S^3 arising from canceling all the differentials.

4.4.2 $D_+(\mu_{1/2}(4_1))$

We now turn our attention to an example computation for the Whitehead double of the dual knot to $1/n$ surgery. Since the surgered 3-manifold is no longer S^3, the expectation is that there will be more than one generator $\alpha \in \widehat{HF}(S^3_{1/n}(K))$ with which to compute τ_α. The immersed curve $\boldsymbol{\alpha}_{4_1}$ is shown in Figure 4.15. Combining α_{4_1} with $\mathcal{H}$ for the Whitehead pattern as seen in Figure 4.10 using the map Φ_2^* as in the proof of Theorem 4.2.12, we arrive at the immersed Heegaard diagram in Figure 4.16. In Figure 4.16, a convenient lift to a suitable covering space was chosen to remove as many immersed points as possible. This way, it is significantly easier to execute the combinatorics of counting discs and to see the generators. From Figure 4.16, we can compute the complex $CFK_{\mathcal{R}}(S^3_{1/n}(K), \mu_{1/n}(K))$ for $K = 4_1$ directly, or simply apply the A-buoy calculus to see the Alexander gradings of the surviving generators after pulling the $\boldsymbol{\beta}$ curve straight, allowing isotopy over z basepoints. In this case, only length one differentials need to be cancelled before arriving at Figure 4.17, where no more useful isotopies can be made. It is clear that only generators $7, 8, 9, 10$, and 11 survive. From the A-buoys, we see that $A(x_7) \neq A(x_8)$, so $\tau_{x_7}(D_+(\mu_{1/n}(K)) \neq \tau_{x_8}(D_+(\mu_{1/n}(K))$, and, in particular, one of them is nonzero. By Corollary 4.3.2, $D_+(\mu_{1/n}(K))$ cannot be slice in $S^3_{1/n}(K) \times I$. Remarkably, if 4_1 were slice in S^3 (it is not), then we could conclude that $D_+(\mu_{1/n}(K))$ is deeply slice in the 4-manifold described in Section 4.1.2, by applying Corollary 4.1.4.

4.5 Proof of Main Theorem

A noteworthy feature of the computation in Example 4.4.2 is that the distinct τ_α-invariants came from generators on the closed component of the immersed curve for the knot. As discussed later, it is suspected this is usually the case. For Theorem 4.0.1, we make use of the fact that its immersed curve has a curve corresponding to a box complex which manifest as a some kind of "8"-looking shape in the immersed curve. Since Theorem 4.0.1 is only for the knot 6_1 as stated, the proof is identical to the computation in Section 4.4.

Proof of Theorem 4.0.1. First, note that $6_1 \subset S^3$ is an alternating, slice knot in B^4. There-
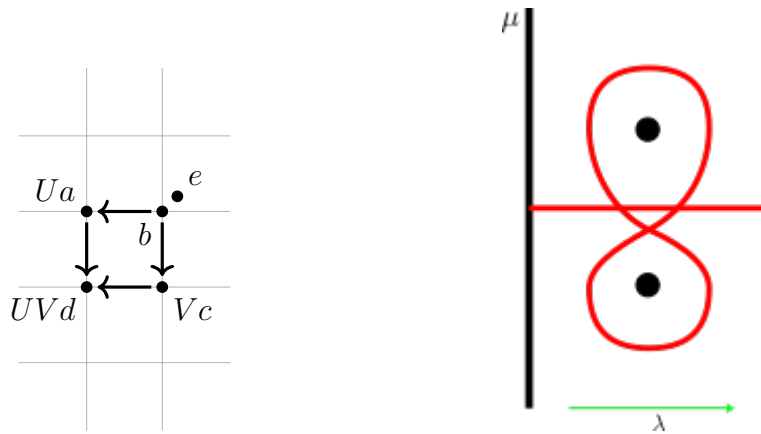
Figure 4.15 Left: A shorthand representation of the complex $CFK_{\mathcal{R}}(4_1)$, the figure eight knot. Right: The immersed curve arising from the complex on the left.
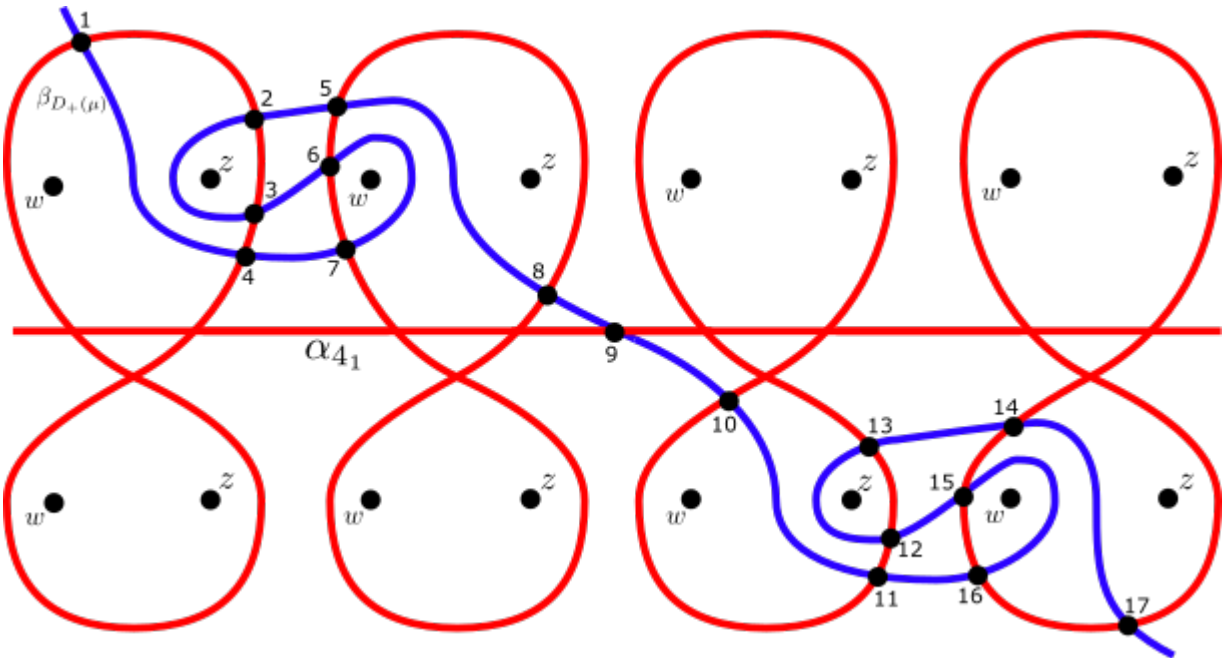

Figure 4.16 A lift of the immersed Heegaard diagram for the pairing of the Whitehead double pattern with the dual knot to $1/2$ surgery along the figure eight knot, 4_1. Notice the change of framing for the Whitehead pattern corresponding to the $1/2$ surgery on 4_1, giving the $\boldsymbol{\beta}$ curve a $-1/2$ slope.
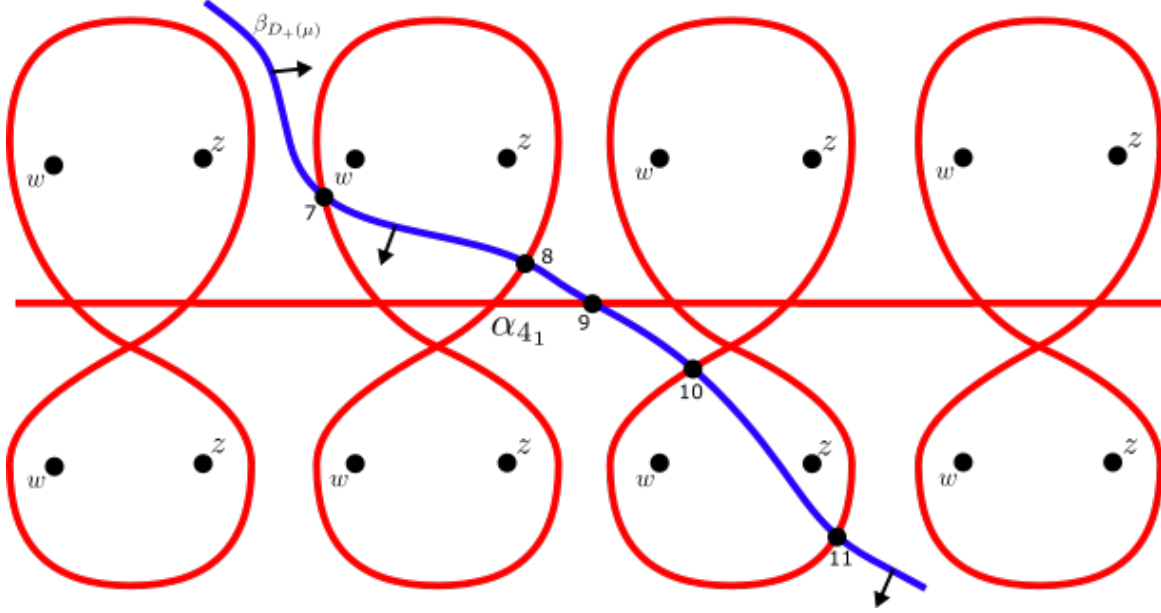
Figure 4.17 The immersed Heegaard diagram arising from canceling all the length one differentials.

fore, $\widehat{HFK}(6_1)$ is determined by its Alexander polynomial, $\Delta_{6_1}(t) = -2t^{-1} + 5 - 2t$, and its signature, $\sigma(6_1) = 0$. By [OS03, theorem 3.1],

$$\widehat{HFK}(S^3, 6_1, A) = \mathbb{F}^2_{-1} \oplus \mathbb{F}^5_0 \oplus \mathbb{F}^2_1,$$

where A is the Alexander grading. Using the spectral sequence from $\widehat{HFK}(6_1)$ to $\widehat{HF}(S^3)$, we can reconstruct the vertical arrows present in the $UV = 0$ knot Floer complex, as in Figure 4.18. Now, using the symmetry granted by swapping the roles of U and V, we reconstruct horizontal arrows in $CFK_{\mathcal{R}}(6_1)$ and plot some more of the generators in the $(\mathrm{gr}_U, \mathrm{gr}_V)$ plane, as in Figure 4.19.

Now that we have the full information $CFK_{\mathcal{R}}(6_1)$ and in a horizontally and vertically simplified basis, we can construct its immersed curve using the method in Proposition 4.2.9, shown in Figure 4.20. Notably, the curve strikingly resembles the curve for 4_1 as in Figure 4.15, with another closed component overlapping the first. Since in Example 4.4.2 only the closed component is necessary to see differing τ_α-invariants, we will only keep track of one of these "8" shapes in the pairing diagram with the bordered Heegaard diagram for the Whitehead double, $\mathcal{H}$. In this case, the local picture near generators x_7 and x_8 in Figure
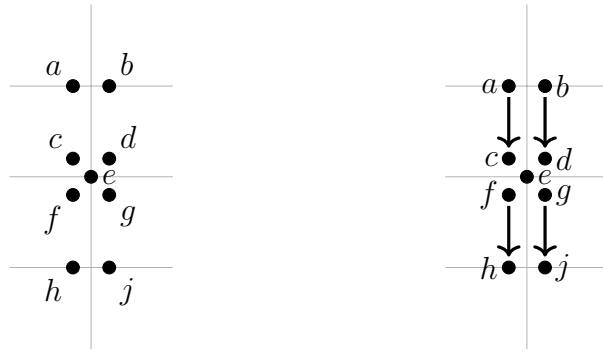
59

Figure 4.18 Left: $\widehat{HFK}(6_1)$ arranged by Alexander grading. Right: the location of the vertical arrows in $CFK_{\mathcal{R}}(6_1)$ if there is to only be one generator for $\widehat{HF}(S^3)$.
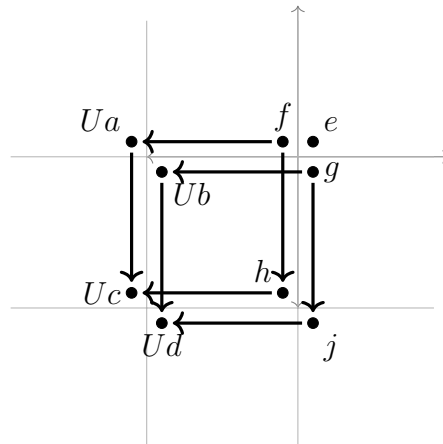

Figure 4.19 Left: adding horizontal arrows in the plane using symmetry along $\mathrm{gr}_U = \mathrm{gr}_V$. Right: a short hand representation of the complex $CFK_{\mathcal{R}}(6_1)$.
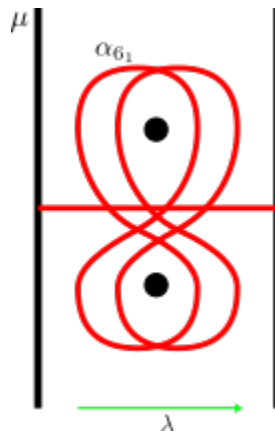

Figure 4.20 The immersed curve for 6_1, $\boldsymbol{\alpha}_{6_1}$.

60

4.16 looks identical (after isotoping away the other curve components) to the local picture for the pairing of $\mathcal{H}$ and $\boldsymbol{\alpha}_{6_1}$. The same two generators, then, still have $\tau_{x_7}(D_+(\mu_{1/n}(K))) \neq \tau_{x_8}(D_+(\mu_{1/n}(K)))$ for $K = 6_1$, so one is nonzero. By Corollary 4.3.2, $D_+(\mu_{1/n}(K))$ cannot be slice in $S^3_{1/n}(K) \times I$. However, since 6_1 is itself slice, Corollary 4.1.4 implies that $D_+(\mu_{1/n}(K))$ is deeply slice in W, the contractible 4-manifold of Proposition 4.1.2. $\quad\square$

BIBLIOGRAPHY

[CH23]   Wenzhao Chen and Jonathan Hanselman, *Satellite knots and immersed heegaard floer homology*, arXiv preprint arXiv:2309.12297 (2023).

[Che23]   Wenzhao Chen, *Knot floer homology of satellite knots with (1, 1) patterns*, Selecta Mathematica **29** (2023), no. 4, 53.

[Dow18]   Nathan Dowlin, *A family of sln-like invariants in knot floer homology*, arXiv preprint arXiv:1804.03165 (2018).

[Dow24]   _____, *A spectral sequence from khovanov homology to knot floer homology*, Journal of the American Mathematical Society (2024).

[Gor75]   C McA Gordon, *Knots, homology spheres, and contractible 4-manifolds*, Topology **14** (1975), no. 2, 151–172.

[GS99]   Robert E Gompf and András Stipsicz, *4-manifolds and kirby calculus*, no. 20, American Mathematical Soc., 1999.

[Han23]   Jonathan Hanselman, *Knot floer homology as immersed curves*, arXiv preprint arXiv:2305.16271 (2023).

[HHSZ22]   Kristen Hendricks, Jennifer Hom, Matthew Stoffregen, and Ian Zemke, *An involutive dual knot surgery formula*, arXiv preprint arXiv:2205.12798 (2022).

[HN13]   Matthew Hedden and Yi Ni, *Khovanov module and the detection of unlinks*, Geometry & Topology **17** (2013), no. 5, 3027–3076.

[HR23]   Matthew Hedden and Katherine Raoux, *Knot floer homology and relative adjunction inequalities*, Selecta Mathematica **29** (2023), no. 1, 7.

[HRW22]   Jonathan Hanselman, Jacob Rasmussen, and Liam Watson, *Heegaard floer homology for manifolds with torus boundary: properties and examples*, Proceedings of the London Mathematical Society **125** (2022), no. 4, 879–967.

[HRW23]   _____, *Bordered floer homology for manifolds with torus boundary via immersed curves*, Journal of the American Mathematical Society (2023).

[Hut02]   Michael Hutchings, *Lecture notes on morse homology (with an eye.*

[Kho00]   Mikhail Khovanov, *A categorification of the jones polynomial.*

[Kir78]   Robion Kirby, *A calculus for framed links in s 3*, Inventiones mathematicae **45** (1978), no. 1, 35–56.

[Kir97]   Rob Kirby, *Problems in low-dimensional topology*, Proceedings 1993 Georgia International Topology Confence, Geometric Topology **2** (1997).

[KR08]   Mikhail Khovanov and Lev Rozansky, *Matrix factorizations and link homology ii*, Geometry & Topology **12** (2008), no. 3, 1387–1425.

[KR21]   Michael Klug and Benjamin Ruppik, *Deep and shallow slice knots in 4-manifolds*, Proceedings of the American Mathematical Society, Series B **8** (2021), no. 17, 204–218.

[Liv05]   Charles Livingston, *A survey of classical knot concordance*, Handbook of knot theory, Elsevier, 2005, pp. 319–347.

[LOT14]   Robert Lipshitz, Peter S Ozsváth, and Dylan P Thurston, *Computing hf by factoring mapping classes*, Geometry & Topology **18** (2014), no. 5, 2547–2681.

[LOT18]   Robert Lipshitz, Peter Ozsváth, and Dylan Thurston, *Bordered heegaard floer homology*, vol. 254, American Mathematical Society, 2018.

[Mil63]   John Willard Milnor, *Morse theory*, no. 51, Princeton university press, 1963.

[ML04]   Khovanov Mikhail and Rozansky Lev, *Matrix factorizations and link homology*.

[MOT09]   Ciprian Manolescu, Peter Ozsváth, and Dylan Thurston, *Grid diagrams and heegaard floer invariants*, arXiv preprint arXiv:0910.0078 (2009).

[OS03]   Peter Ozsváth and Zoltán Szabó, *Heegaard floer homology and alternating knots*, Geometry & Topology **7** (2003), no. 1, 225–254.

[OS04a]   _____, *Heegaard diagrams and holomorphic disks*, Different faces of geometry, Springer, 2004, pp. 301–348.

[OS04b]   _____, *Holomorphic disks and knot invariants*, Advances in Mathematics **186** (2004), no. 1, 58–116.

[OS04c]   _____, *Holomorphic disks and three-manifold invariants: properties and applications*, Annals of Mathematics (2004), 1159–1245.

[OS04d]   _____, *Holomorphic disks and topological invariants for closed three-manifolds*, Annals of Mathematics (2004), 1027–1158.

[OS05a]   _____, *On knot floer homology and lens space surgeries*, Topology **44** (2005), no. 6, 1281–1300.

[OS05b]   _____, *On the heegaard floer homology of branched double-covers*, Advances in Mathematics **194** (2005), no. 1, 1–33.

[Pet13]   Ina Petkova, *Cables of thin knots and bordered heegaard floer homology*, Quantum Topology **4** (2013), no. 4, 377–409.

[Ras03]   Jacob Andrew Rasmussen, *Floer homology and knot complements*, Harvard University, 2003.

[Ras05]   Jacob Rasmussen, *Knot polynomials and knot homologies*, arXiv preprint math/0504045 (2005).

[Sav11] Nikolai Saveliev, *Lectures on the topology of 3-manifolds: an introduction to the casson invariant*, Walter de Gruyter, 2011.

[SW10] Sucharit Sarkar and Jiajun Wang, *An algorithm for computing some heegaard floer homologies*, Annals of mathematics (2010), 1213–1236.

[Tur97] Vladimir Turaev, *Torsion invariants of spin^c-structures on 3-manifolds*, Mathematical Research Letters **4** (1997), no. 5, 679–695.